# Some SERS Fingerprints of Metabolites from the Database provided by Sherman et al., 2020

**Amelia Carolina Sparavigna**

Department of Applied Science and Technology, Polytechnic University of Turin, Turin, Italy

Torino, November 16, 2023

**Abstract:** This research work is proposing the fingerprints of some SERS (Surface-Enhanced Raman) spectra of metabolites, published by Sherman et al. in 2020. The fingerprints are those of Bis(3-Aminopropyl)Amine, Caffeine, Cys-Gly, Cysteamine, Cytochrome C, Dihydrofolate, Histamine, Homocysteine, Homocystine, Kynurenine, L-Arginine, L-Cysteine, L-Cystine, L-Lysine, L-Tryptophan, N-Acetyl-L-Cysteine, Nicotinamide, Octopamine, Selenocystamine, Tetrahydrofolate, and Thiamine. Comparison with other data from literature are proposed for Cysteamine and L-Cysteine. Very interesting are the SERS fingerprints of Homocysteine, Homocystine, L-cysteine and L-cystine, because we can easily identify the common SERS bands.

In a previous work [1], we have considered three of the Surface-Enhanced Raman spectra of metabolites proposed in [2] by Sherman et al.,2020, to investigate the line shapes of the measured peaks. The metabolites were L-Cysteine, Cysteamine and Homocysteine, and the SERS peaks were fitted by means of the Tsallis q-Gaussian functions. These functions are considered by the author (AC Sparavigna) as fundamental for any deconvolution of Raman spectra, as shown by several cases (see for instance, [3]-[8]). Here we consider again some of the SERS spectra of metabolites given in [2], to show the importance of gaining information from their fingerprints.

The first use of the term "fingerprint" in relation with the Raman spectroscopy, to the best of my knowledge, is in an article published in 1947, about the Raman spectra of hydrocarbons [9]. Fenske et al., 1947, wrote that the bands of the Raman spectrum, "which are called Raman lines, are characteristic of the substance illuminated and are therefore a "fingerprint" of that substance". From that time on, the points of identification, such as positions of peaks, shoulders and valleys are creating the characteristic spectral pattern which is defined as the "Raman fingerprint" of a given material. This pattern allows the material classification, "without any preliminary information about composition and structural origin of the individual features", as mentioned by D'Ippolito, et al., 2015 [10].

In [11], we proposed a method based on the first derivative behavior, that is on the "first derivative spectrum" [12], to determine the position of the peaks. Details of the method are provided in [11]. As previously told, here we apply it to determine some of the SERS fingerprints of the metabolites, the spectra of which have been kindly provided by Sherman et al., 2020. The authors of this fundamental research have also provided a document with chemical formulae, spectra, and also useful references. Thanks to this precious support, we can propose the related fingerprints.

The Table S1 by Sherman et al. is showing the SERS Metabolites organized in alphabetical order, with their classification, and the page where formulae and spectra are provided. Here we use the

same alphabetic order, providing some fingerprints in the form of spectra and tables. We investigate a part of the spectra, because the main aim of the work is that of pointing out the importance of the proposed database and of the fingerprint method for identifying the relevant spectral bands.

The metabolites here investigated are the following:

| METABOLITE | CLASSIFICATION |
|---|---|
| Bis(3-Aminopropyl)Amine | Polyamine |
| Caffeine | Stimulant |
| Cys-Gly | Peptide |
| Cysteamine | Antioxidant |
| Cytochrome C | Protein |
| Dihydrofolate | Vitamin |
| Histamine | Neurotransmitter |
| Homocysteine | Amino Acid Analog |
| Homocystine | Amino Acid Analog |
| Kynurenine | Carboxylic Acid |
| L-Arginine | Amino Acid |
| L-Cysteine | Amino Acid |
| L-Cystine | Antioxidant |
| L-Lysine | Amino Acid |
| L-Tryptophan | Amino Acid |
| N-Acetyl-L-Cysteine | Antioxidant |
| Nicotinamide | Vitamin |
| Octopamine | Neurotransmitter |
| Selenocystamine | Polyamine |
| Tetrahydrofolate | Coenzyme |
| Thiamine | Vitamin |

In the plots we will propose, the blue line is representing the intensity threshold, above which the peak is considered relevant for the fingerprint. Of course, the value of the threshold can be changed when specific comparisons among fingerprints are necessary. Below the plots, tables with the positions of the peaks and the relative intensity are provided. Note that the peaks given by Sherman et al., have intensity scaled to 1. In the method to evaluate the peak positions, some data smoothing is necessary, so the intensity of the main peak can be slightly lower than the unit value. For what is regarding the uncertainty of the peak position, we must note that spacing of the data provided by Sherman et al. is of about 2 $cm^{-1}$, and therefore the uncertainty is estimated to be plus/minus 2 $cm^{-1}$. In the figure captions, the references given by Sherman et al. are also maintained, and further literature added. In some of the spectra, we have also provided the chemical formula as illustrated by Sherman et al., 2020.

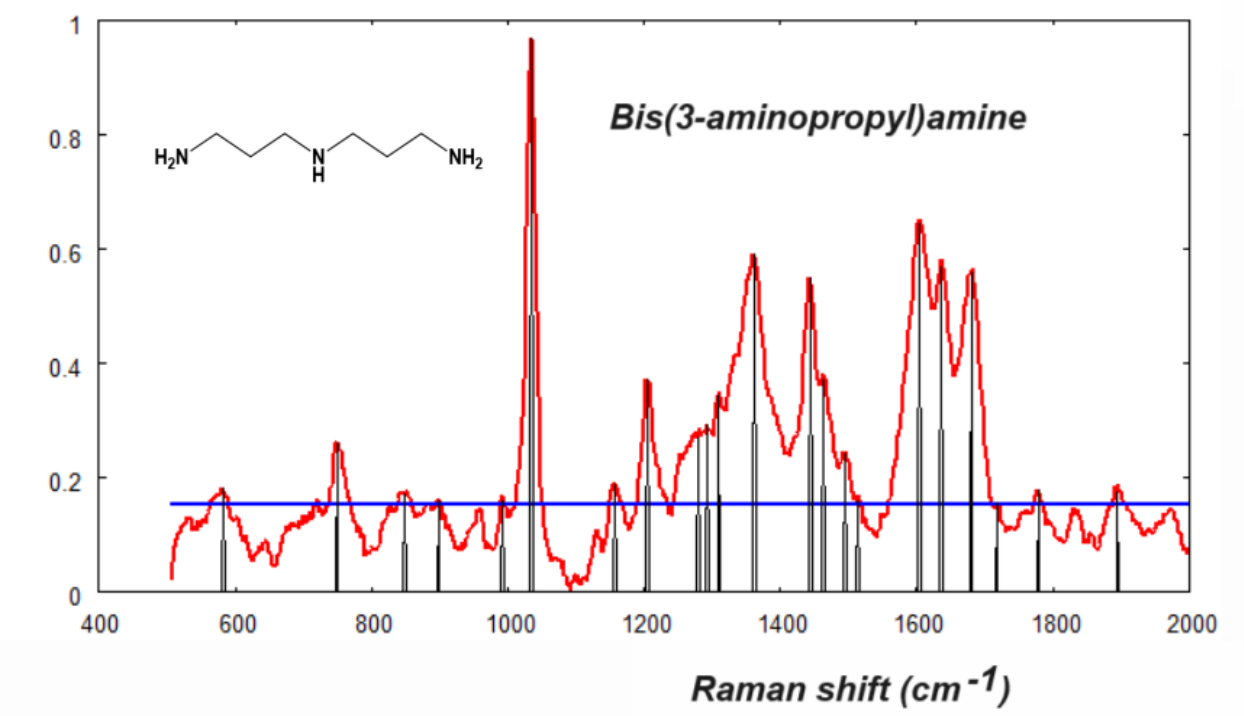


| Position (in $cm^{-1}$) | Relative intensity | Position (in $cm^{-1}$) | Relative intensity |
|---|---|---|---|
| 581.50 | 0.18 | 1361.50 | 0.59 |
| 749.00 | 0.26 | 1444.00 | 0.55 |
| 849.00 | 0.17 | 1462.50 | 0.37 |
| 897.50 | 0.16 | 1495.00 | 0.24 |
| 991.50 | 0.16 | 1513.00 | 0.16 |
| 1035.00 | 0.97 | 1604.00 | 0.64 |
| 1157.50 | 0.19 | 1636.00 | 0.57 |
| 1204.00 | 0.37 | 1680.00 | 0.56 |
| 1280.00 | 0.27 | 1717.50 | 0.16 |
| 1292.50 | 0.29 | 1778.00 | 0.18 |
| 1309.50 | 0.34 | 1894.50 | 0.17 |

**Main peak at 1035 $cm^{-1}$.**

**Figure 1.** SERS spectrum and fingerprint of bis(3-aminopropyl)amine. Let us suggest the article by Dongil et al., 2014, about the insertion of bis (3-aminopropyl) amine into graphite oxide [13].

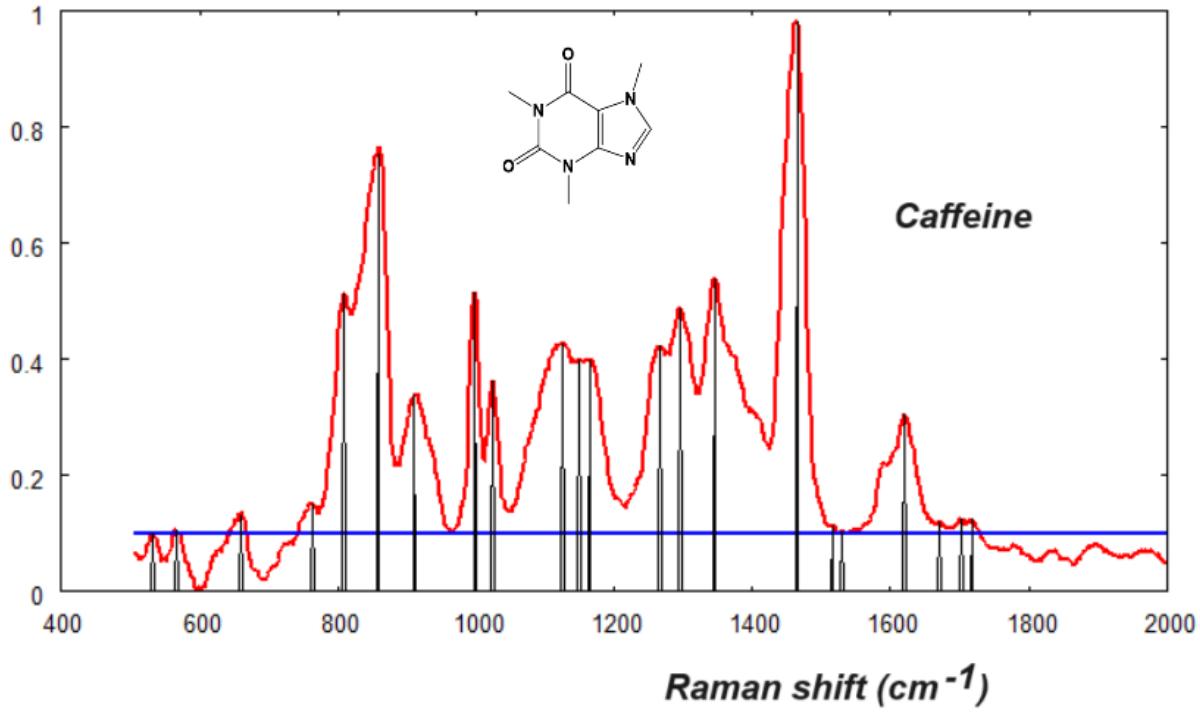


| Position (in $cm^{-1}$) | Relative intensity | Position (in $cm^{-1}$) | Relative intensity |
|---|---|---|---|
| 531.50 | 0.10 | 1164.00 | 0.40 |
| 565.50 | 0.11 | 1265.50 | 0.42 |
| 659.00 | 0.13 | 1294.50 | 0.49 |
| 762.50 | 0.15 | 1344.50 | 0.54 |
| 809.00 | 0.51 | 1464.50 | 0.98 |
| 858.00 | 0.75 | 1515.00 | 0.11 |
| 911.00 | 0.34 | 1529.50 | 0.10 |
| 998.00 | 0.51 | 1620.00 | 0.31 |
| 1024.00 | 0.36 | 1670.00 | 0.12 |
| 1125.50 | 0.43 | 1701.50 | 0.12 |
| 1149.00 | 0.40 | 1717.50 | 0.12 |

**Main peak at 1464.5 $cm^{-1}$.**

**Figure 2.** SERS spectrum and fingerprint of caffeine. SERS spectra have previously been reported (Sherman et al.) in the literature [14],[15],[16]. Let us add [17],[18],[19],[20],[21].

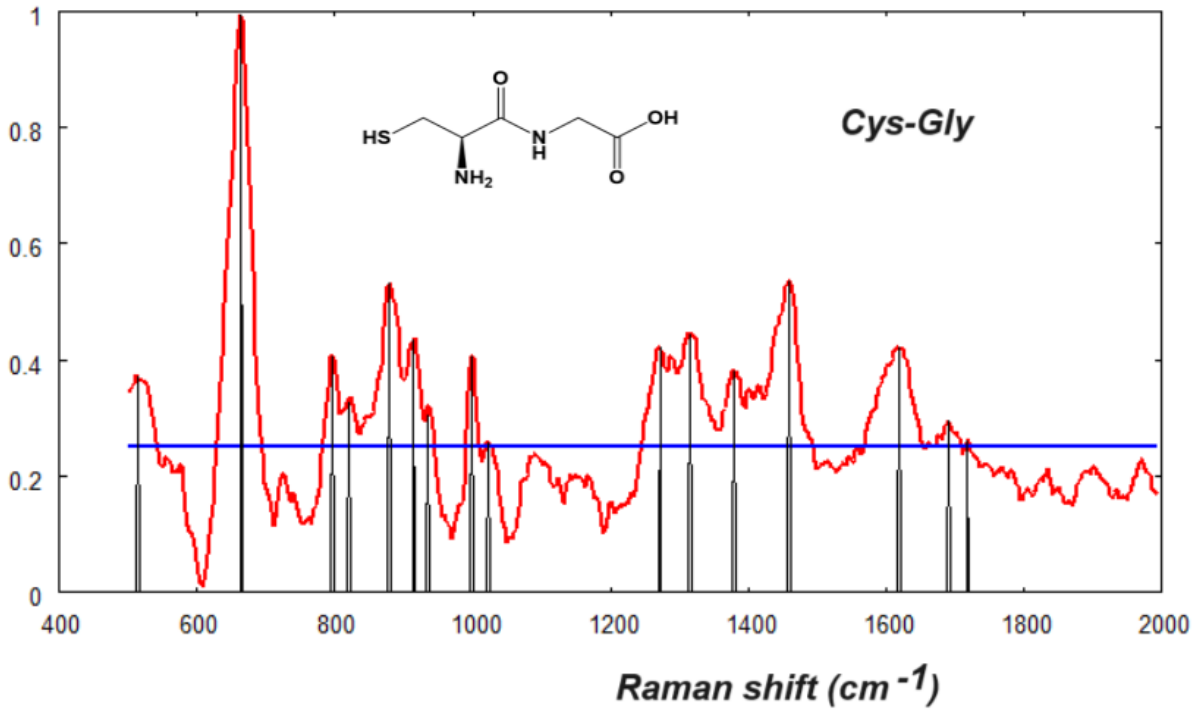


| Position (in cm -1) | Relative intensity | Position (in cm -1) | Relative intensity |
|---|---|---|---|
| 514.00 | 0.37 | 1023.00 | 0.26 |
| 663.50 | 0.99 | 1271.50 | 0.42 |
| 795.50 | 0.40 | 1315.50 | 0.44 |
| 820.00 | 0.33 | 1379.50 | 0.38 |
| 879.50 | 0.53 | 1460.00 | 0.53 |
| 914.50 | 0.44 | 1619.50 | 0.42 |
| 934.00 | 0.30 | 1691.00 | 0.29 |
| 999.00 | 0.41 | 1718.50 | 0.26 |

**Main peak at 663.5 $cm^{-1}$.**

**Figure 3.** SERS spectrum and fingerprint of L-cysteine-L-glycine (Cys-Gly). Literature (Sherman et al.) for this molecule [22]. Let us here add literature about L-methionine (Met), L-cysteine (Cys), L-glycine (Gly), L-leucine (Leu), L-phenylalanine (Phe), L-proline (Pro) and their homodipeptides Met-Met, Cys-Cys, Gly-Gly, LeuLeu, Phe-Phe, and Pro-Pro [23].

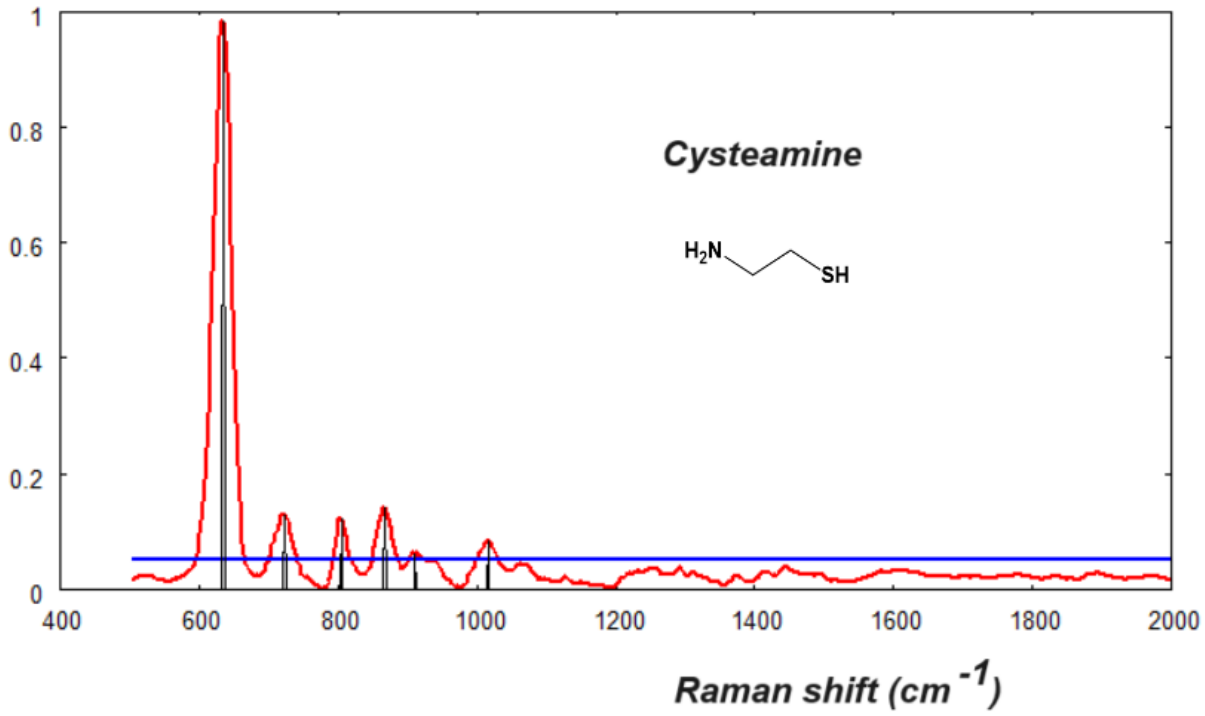


| Position (in cm -1) | Relative intensity |
|---|---|
| 634.00 | 0.98 |
| 721.00 | 0.13 |
| 804.50 | 0.12 |
| 866.50 | 0.14 |
| 910.00 | 0.06 |
| 1015.50 | 0.08 |

**Main peak at 634.0 $cm^{-1}$.**

**Figure 4a.** SERS spectrum and fingerprint of cysteamine. Literature (Sherman et al.) for this molecule [24],[25],[26],[27],[28]. Let us add [29].

In the following Table I, we show the peaks as determined by means of the q-Gaussian deconvolution, proposed in [1], where the data by Sherman et al. have been used too. We can observe some slight differences in peak positions, generated by the deconvolution approach. However, differences are within the uncertainty of plus/minus 2 $cm^{-1}$. The other data considered are those from literature mentioned by Sherman et al. and from Ref. [29]. The position of the peaks is given in $cm^{-1}$.

| | | | | | | | | | | | | | |
|---|---|---|---|---|---|---|---|---|---|---|---|---|---|
| From Fig. 4a | | 634 | 721 | 804.5 | | 866.5 | 910 | | 1015.5 | | | | |
| Sherman et al., 2020. | 613 | 633 | 719 | 803.5 | 823.5 | 865.5 | 908 | 936.5 | 1014 | 1064 | 1094 | 1126.5 | 1150 |
| Jiang et al., 2013, Cys/silver | 387 | | 640 | | 831 | | | 978 | 1047 | | | | |
| Jiang et al., 2013, Cys powder | 510 | | 661 | 793 | | | | 984 | 1045 | | | | |
| Kudelski and Hill, 1999, Cys solid | | | | 758 | | | | 938 | 1012 | | | | |
| Kudelski and Hill, 1999, Cys sol | 510 | | 666 | 753 | 817 | | | 936 | 1013 | | | | |
| Kudelski and Hill, 1999, Cys mono | 509 | | 640 | 726 | | | | 946 | 1014 | | | | |
| Kudelski and Hill, 1999, Cys mono | | | 640 | 725 | | | | 940 | 1013 | | | | |

Table I.

Here in the following plot, it is given the Figure 9 in [1]. Other plots and discussion in [1].

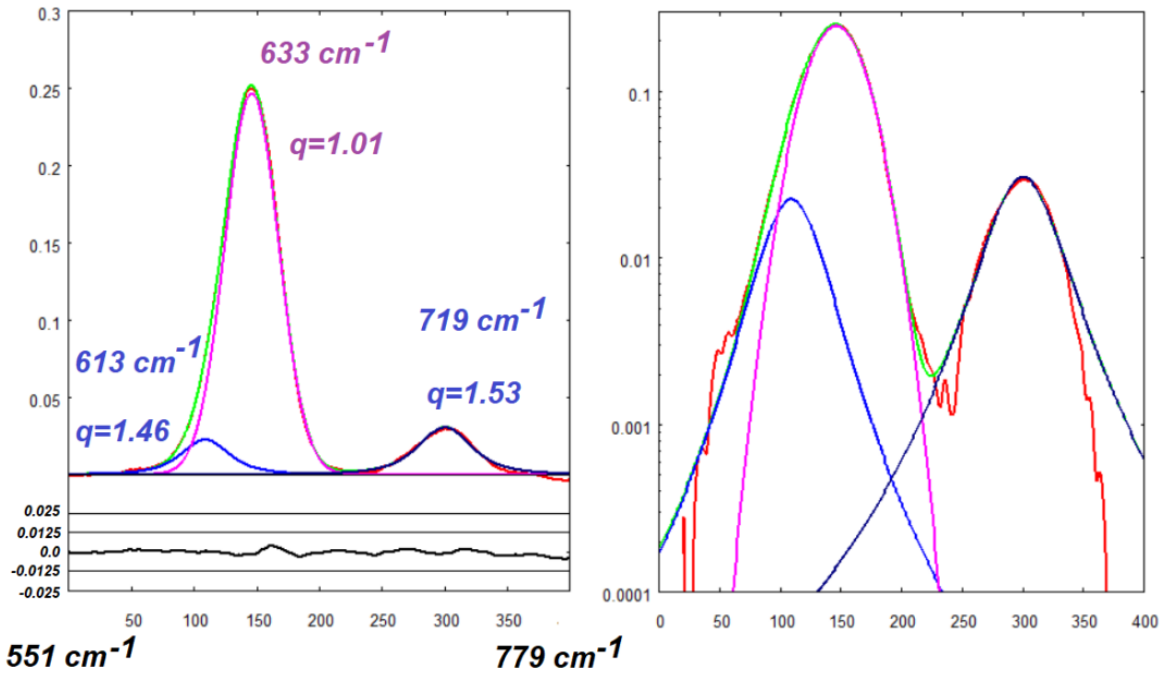


**Fig. 4b.** Fitting (green) onto data (red) of Cysteamine (data Sherman et al., 2020). Frequency ranges from 781.5 to 973.5 $cm^{-1}$. For the deconvolution, five q-Gaussians are used (values of the q-parameters are given in the figure). On the right, the plot is given in the semi log scale. The q-Gaussian center positions are 803.5, 823.5, 865.5, 908 and 936.5 $cm^{-1}$, from left to right.

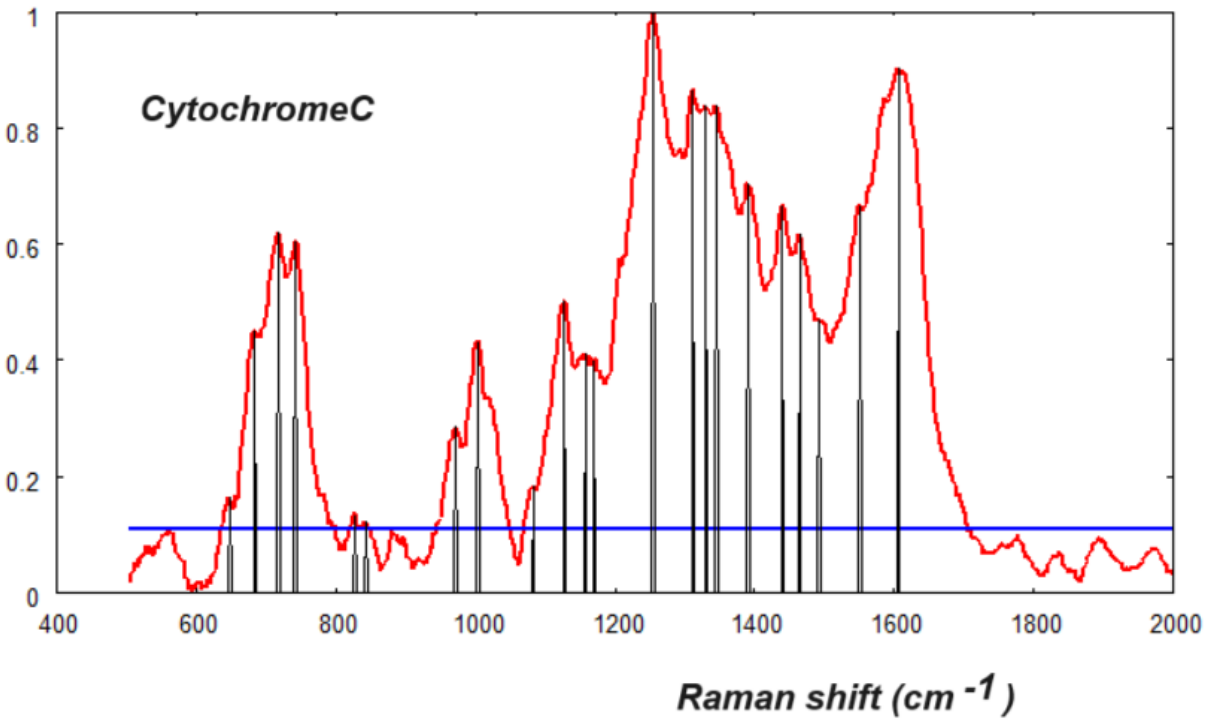


| Position (in cm$^{-1}$) | Relative intensity | Position (in cm$^{-1}$) | Relative intensity |
|---|---|---|---|
| 647.50 | 0.16 | 1170.00 | 0.40 |
| 683.50 | 0.45 | 1255.00 | 1.00 |
| 717.50 | 0.62 | 1311.50 | 0.86 |
| 742.00 | 0.60 | 1330.00 | 0.84 |
| 827.00 | 0.13 | 1344.50 | 0.84 |
| 842.50 | 0.12 | 1390.50 | 0.70 |
| 972.00 | 0.28 | 1439.50 | 0.66 |
| 1002.50 | 0.43 | 1464.50 | 0.62 |
| 1082.50 | 0.18 | 1493.00 | 0.47 |
| 1127.50 | 0.50 | 1551.50 | 0.66 |
| 1157.50 | 0.41 | 1606.00 | 0.90 |

**Main peak at 1255.0 cm$^{-1}$.**

**Figure 5.** SERS spectrum and fingerprint of cytochrome C. Literature reported for this molecule by Sherman et al. are [30],[31]. Let us add [32],[33].

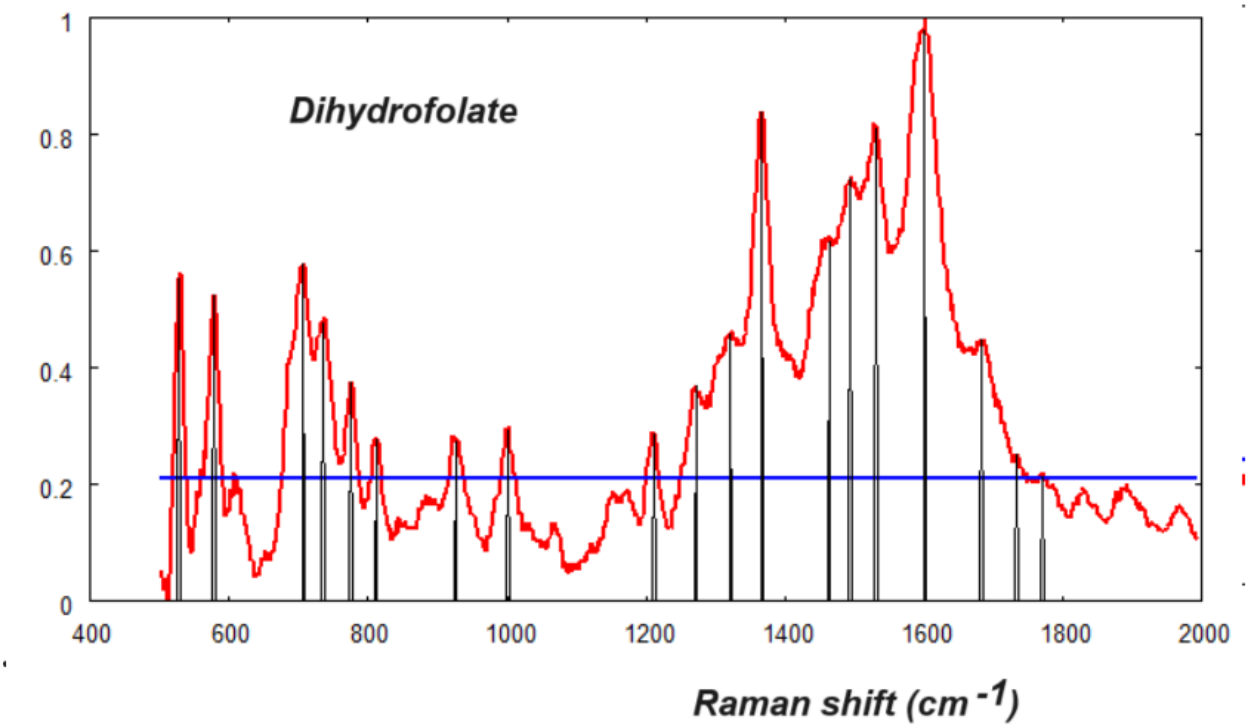


| Position (in cm -1) | Relative intensity | Position (in cm -1) | Relative intensity |
|---|---|---|---|
| 527.50 | 0.55 | 1321.50 | 0.46 |
| 577.50 | 0.53 | 1367.50 | 0.84 |
| 706.50 | 0.58 | 1464.00 | 0.62 |
| 735.50 | 0.47 | 1494.50 | 0.72 |
| 775.50 | 0.38 | 1531.00 | 0.81 |
| 811.00 | 0.28 | 1601.50 | 0.98 |
| 925.50 | 0.27 | 1683.00 | 0.45 |
| 1001.50 | 0.29 | 1734.00 | 0.25 |
| 1210.50 | 0.29 | 1771.50 | 0.21 |
| 1271.50 | 0.37 | | |

**Main peak at 1601.5 $cm^{-1}$.**

**Figure 6.** SERS spectrum and fingerprint of dihydrofolate. No references given by Sherman et al.

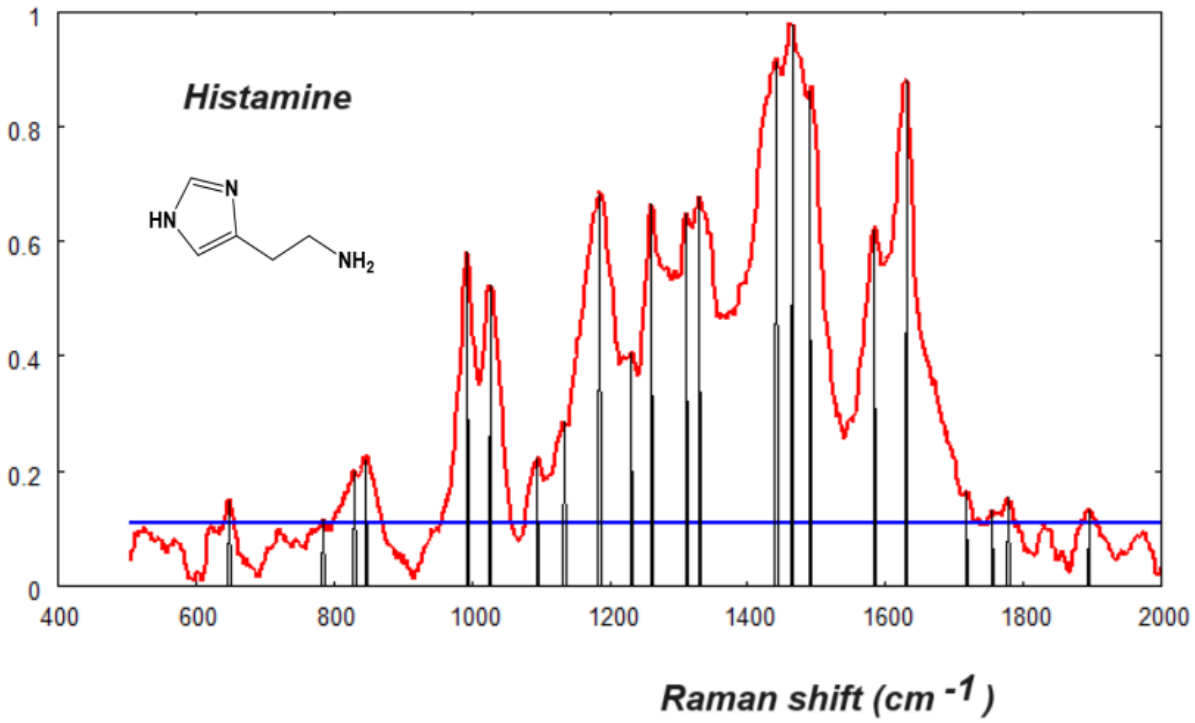


| Position (in cm -1) | Relative intensity | Position (in cm -1) | Relative intensity |
|---|---|---|---|
| 647.50 | 0.15 | 1311.50 | 0.65 |
| 784.50 | 0.11 | 1330.00 | 0.68 |
| 829.00 | 0.20 | 1442.00 | 0.91 |
| 847.00 | 0.22 | 1464.50 | 0.98 |
| 994.00 | 0.58 | 1491.00 | 0.86 |
| 1026.50 | 0.52 | 1584.00 | 0.62 |
| 1095.50 | 0.22 | 1630.00 | 0.88 |
| 1134.00 | 0.28 | 1717.50 | 0.16 |
| 1185.00 | 0.68 | 1755.00 | 0.13 |
| 1231.50 | 0.40 | 1778.00 | 0.15 |
| 1261.00 | 0.66 | 1894.50 | 0.13 |

**Main peak at 1464.5 $cm^{-1}$.**

**Figure 7.** SERS spectrum and fingerprint of histamine. SERS spectra reported by Sherman et al. are [35],[36],[37]. Let us add [38],[39],[40],[41].

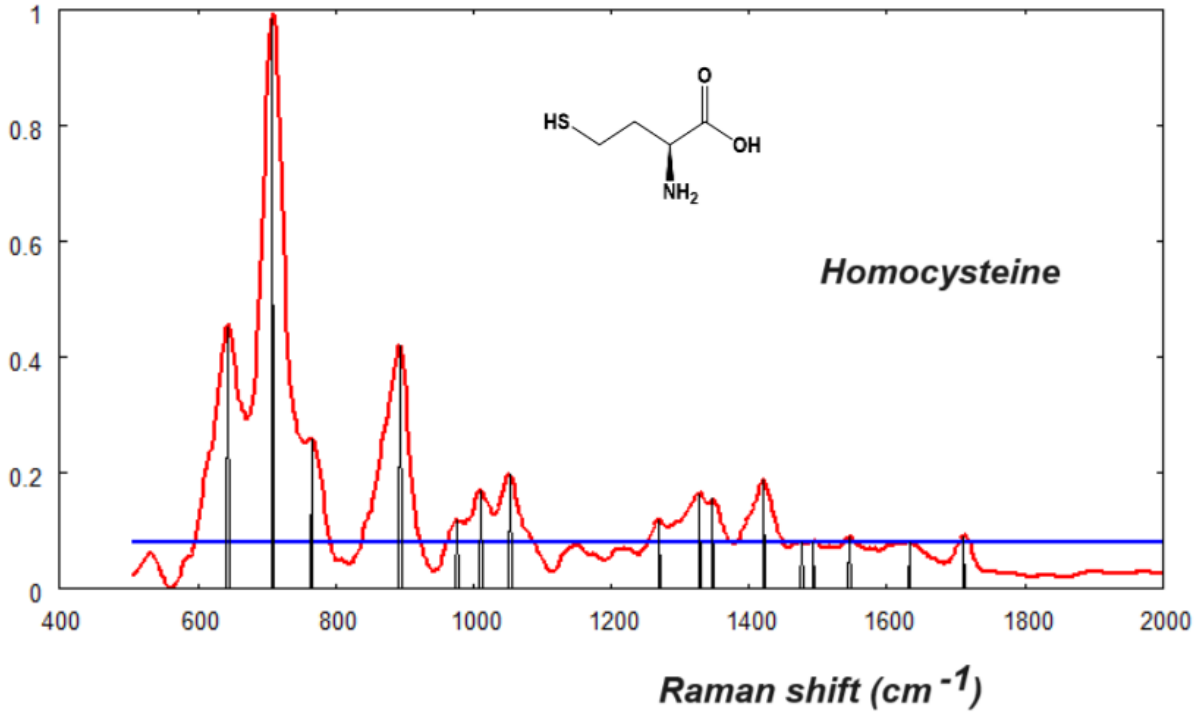


| Position (in cm$^{-1}$) | Relative intensity | Position (in cm$^{-1}$) | Relative intensity |
|---|---|---|---|
| 643.00 | 0.45 | 1328.00 | 0.16 |
| 708.50 | 0.98 | 1347.00 | 0.16 |
| 764.50 | 0.26 | 1421.00 | 0.19 |
| 893.00 | 0.42 | 1476.50 | 0.08 |
| 976.50 | 0.12 | 1493.00 | 0.08 |
| 1011.00 | 0.17 | 1545.50 | 0.09 |
| 1052.50 | 0.20 | 1632.00 | 0.08 |
| 1269.50 | 0.12 | 1711.50 | 0.09 |

**Main peak at 708.5 cm$^{-1}$.**

**Figure 8.** SERS spectrum and fingerprint of homocysteine. No reference is given by Sherma et al., so let us mention Zheng et al., 2023 [42].

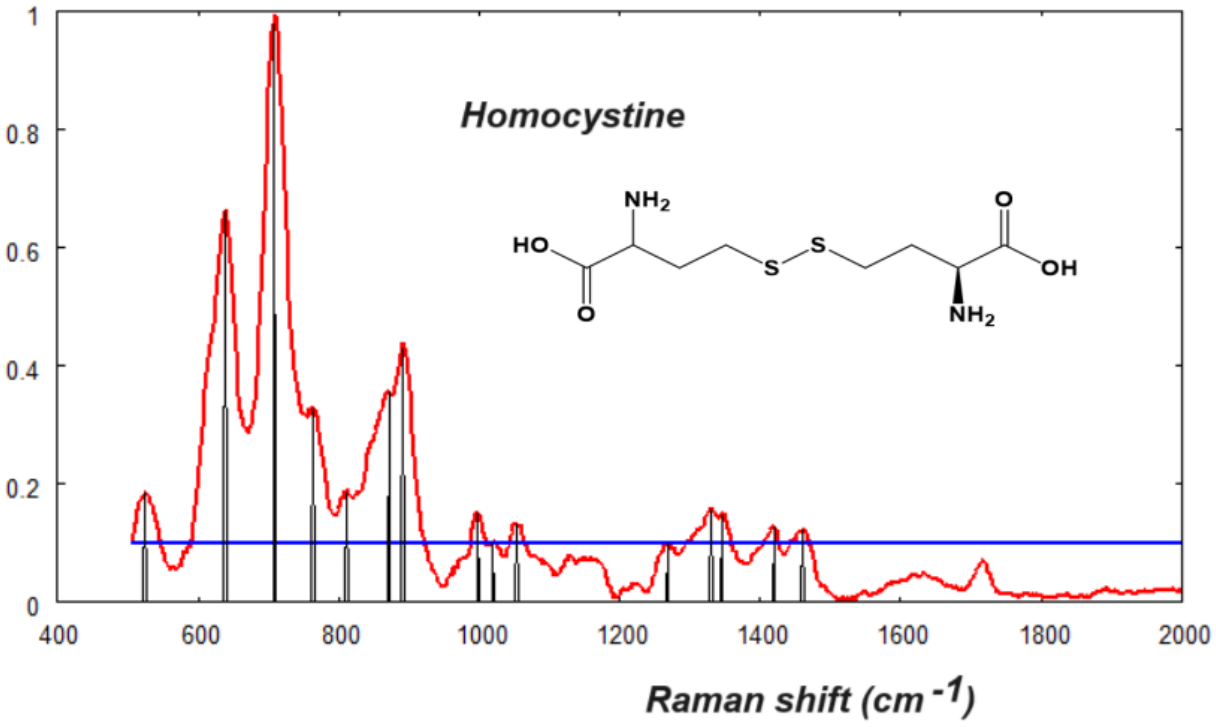


| Position (in cm -1) | Relative intensity | Position (in cm -1) | Relative intensity |
|---|---|---|---|
| 524.50 | 0.18 | 1020.00 | 0.10 |
| 638.50 | 0.66 | 1052.50 | 0.13 |
| 708.50 | 0.98 | 1267.50 | 0.10 |
| 762.50 | 0.33 | 1330.00 | 0.16 |
| 811.50 | 0.19 | 1344.50 | 0.15 |
| 871.00 | 0.35 | 1419.00 | 0.13 |
| 891.00 | 0.43 | 1460.00 | 0.12 |
| 998.00 | 0.15 | | |

**Main peak at 708.5 $cm^{-1}$.**

**Figure 9.** SERS spectrum and fingerprint of homocystine. No reference is given by Sherman et al.

It is interesting to observe the two SERS spectra of homocysteine and homocystine together as in the following plot.

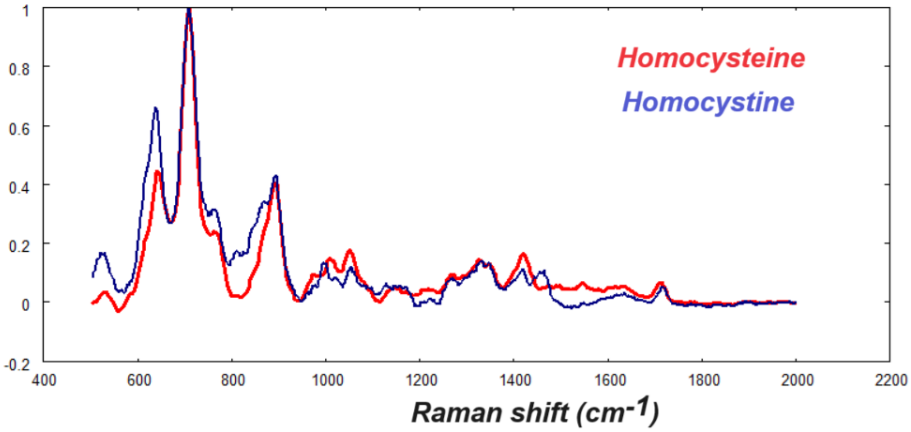


According to the fingerprints given in Figs. 8 and 9:

| | | | | | | | | | | | |
|---|---|---|---|---|---|---|---|---|---|---|---|
| Homocysteine | | 643 | 708.5 | 764.5 | | | 893 | 976.5 | 1011 | | |
| Homocystine | 524.5 | 638.5 | 708.5 | 762.5 | 811.5 | 871 | 891 | 998 | 1020 | | |

| | | | | | | | | | | |
|---|---|---|---|---|---|---|---|---|---|---|
| Homocysteine | 1052.5 | 1269.5 | 1328 | 1347 | 1421 | 1476.5 | 1493 | 1545.5 | 1632 | 1711.5 |
| Homocystine | 1052.5 | 1267.5 | 1330 | 1344.5 | 1419 | 1460 | | | | |

To improve the comparison, let us reduce the threshold in the case of homocystine, as in the following plot.

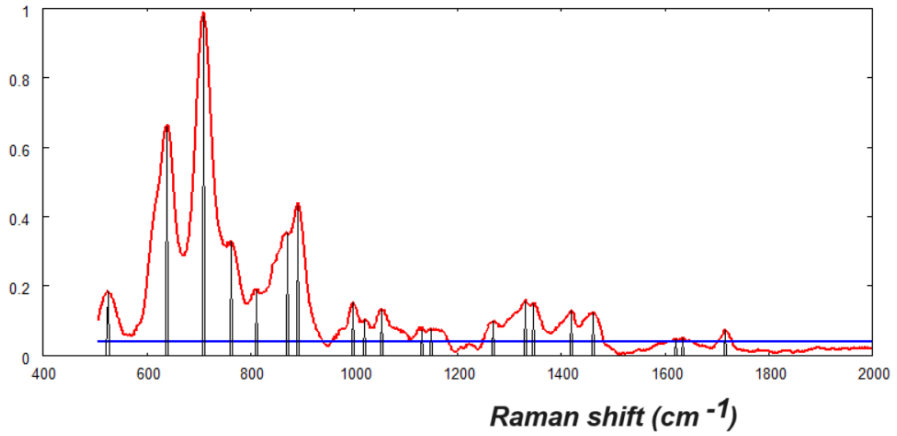


According to the new fingerprint of homocystine (within the uncertainty of plus/minus 2 $cm^{-1}$.):

| | | | | | | | | | | | |
|---|---|---|---|---|---|---|---|---|---|---|---|
| Homocysteine | | 643 | **708.5** | **764.5** | | | **893** | 976.5 | 1011 | | |
| Homocystine | 524.5 | 638.5 | **708.5** | **762.5** | 811.5 | 871 | **891** | 998 | 1020 | | |

| | | | | | | | | | | | |
|---|---|---|---|---|---|---|---|---|---|---|---|
| Homocysteine | **1052.5** | | | **1269.5** | **1328** | **1347** | **1421** | 1476.5 | 1493 | 1545.5 | **1632** | **1711.5** |
| Homocystine | **1052.5** | 1129.5 | 1149 | **1267.5** | **1330** | **1344.5** | **1419** | 1460 | | 1620 | **1634** | **1715.5** |

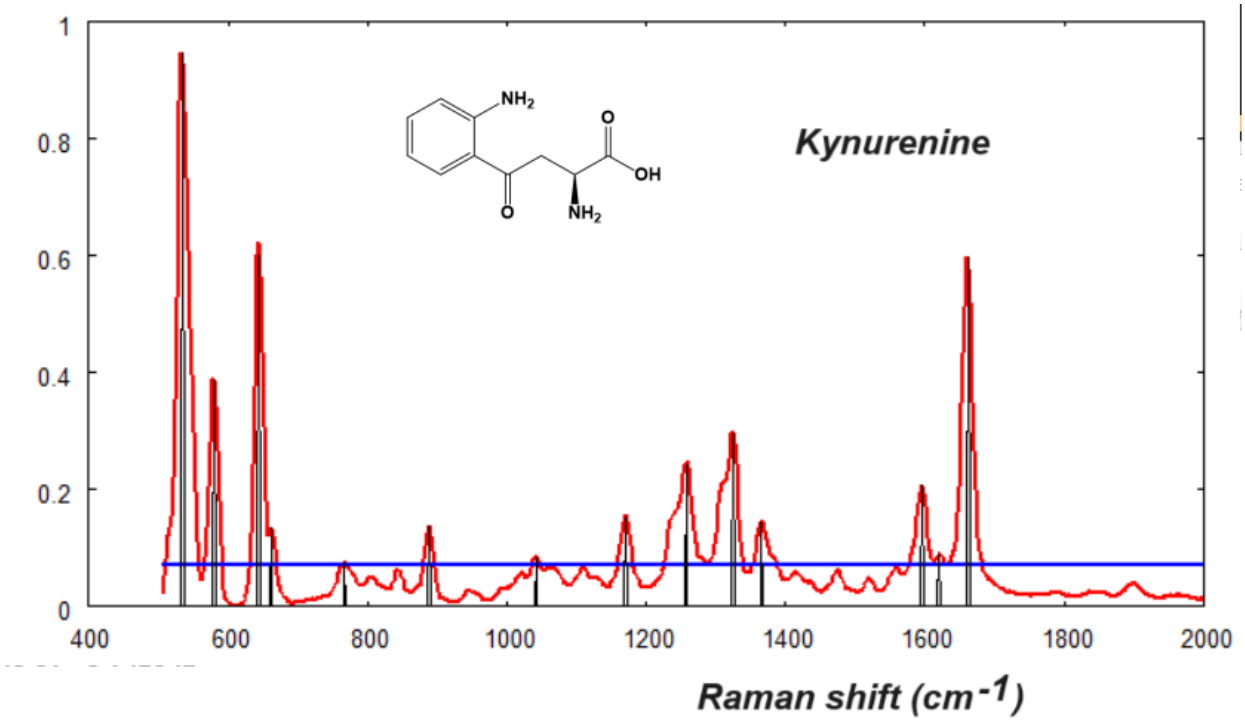


| Position (in $cm^{-1}$) | Relative intensity | Position (in $cm^{-1}$) | Relative intensity |
|---|---|---|---|
| 533.50 | 0.94 | 1170.00 | 0.15 |
| 579.50 | 0.39 | 1257.00 | 0.24 |
| 643.00 | 0.60 | 1324.00 | 0.30 |
| 661.00 | 0.13 | 1365.50 | 0.14 |
| 767.00 | 0.07 | 1596.00 | 0.21 |
| 889.00 | 0.14 | 1620.00 | 0.09 |
| 1041.50 | 0.08 | 1662.00 | 0.60 |

**Main peak at 533.5 $cm^{-1}$.**

**Figure 10.** SERS spectrum and fingerprint of kynurenine. As told by Sherman et al., SERS spectra have previously been reported for this molecule [43].

Let us add here a discussion from the recent work by Das et al., 2021 [44]. The abstract of their review is proposing the Surface-Snhanced Raman spectroscopy (SERS) as "a powerful tool for biosensing applications owing to its *fingerprint recognition*, high sensitivity, multiplex detection, and biocompatibility" [44]. According to the authors, their review is offering "an overview of the most significant aspects of SERS for biomedical and biosensing applications" [44].
In the review, kynurenine is mentioned as follow. "Intrinsic SERS signals can be used to detect specific biomarkers or physiologically relevant biomolecular species inside or near individual cells, such as important metabolites in normal and tumor cells, or other cellular components such as exosomes. The application of SERS to identify the presence of extracellular metabolites, secreted by cancer cells and relevant to tumor biology, including tryptophan, *kynurenine*, and purine derivatives, has been demonstrated by Plou et al. " ([44] is mentioning [45]).
In Figure 7 of Ref. [44], the Panel (e) allows a "comparison of Raman and SERS spectra for kynurenine (Kyn) and tryptophan (Trp)". The panel is reproducing from Wiley publication [45]. The nanoparticles are of gold.
From the plot by Plou et al., [44],[45], we can obtain the peaks above a certain threshold at positions that we can compare with those given by Sherman et al. (in $cm^{-1}$):

| | | | | | | | | | | | |
|---|---|---|---|---|---|---|---|---|---|---|---|
| *Plou et a.* | *562.5* | | *664.0* | | *938.0* | *999.5* | *1039.5* | | *1227.0* | *1350.5* | *1378.0* |
| *Sherman et al.* | *533.5* | *579.5* | *643.0* | *661.0* | *767.0* | *889.0* | *1041.5* | *1170.0* | *1257.0* | *1324.0* | *1365* |

In Plou et al., the main peak is at 562.5 $cm^{-1}$.

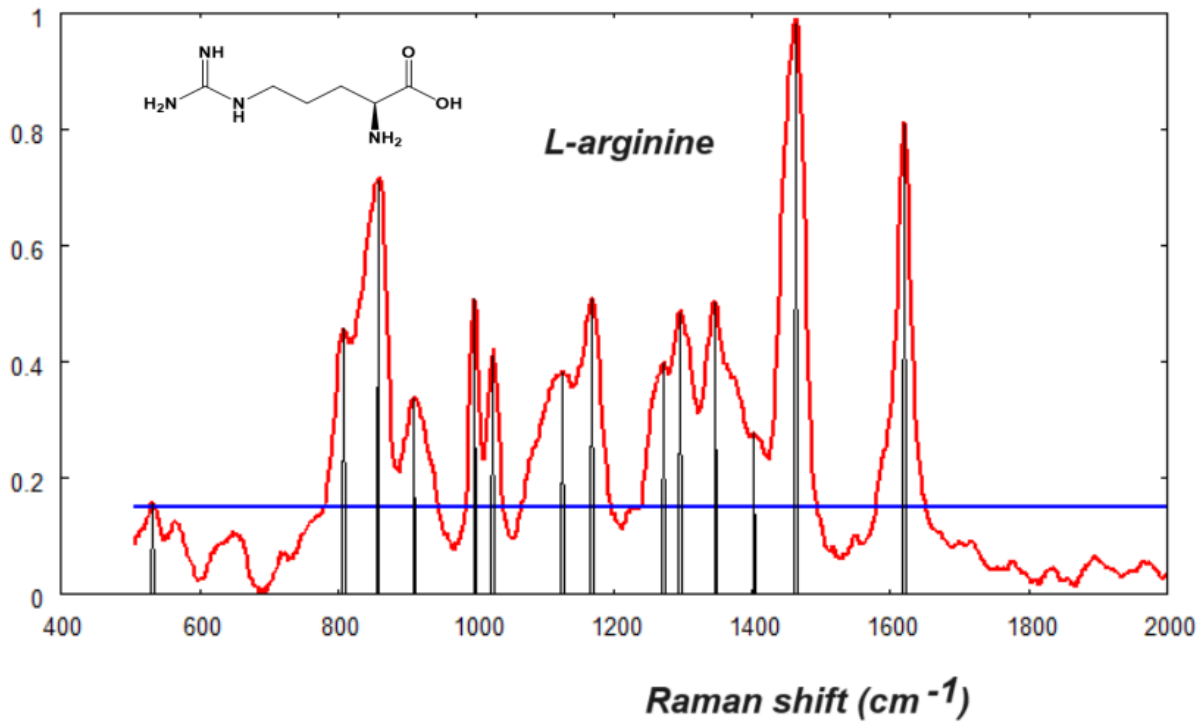


| Position (in cm -1) | Relative intensity | Position (in cm -1) | Relative intensity |
|---|---|---|---|
| 531.50 | 0.16 | 1168.00 | 0.51 |
| 809.00 | 0.46 | 1271.50 | 0.40 |
| 858.00 | 0.71 | 1294.50 | 0.48 |
| 911.00 | 0.34 | 1347.00 | 0.50 |
| 998.00 | 0.51 | 1402.50 | 0.28 |
| 1024.00 | 0.41 | 1462.50 | 0.98 |
| 1125.50 | 0.38 | 1620.00 | 0.81 |

**Main peak at 1462.5 $cm^{-1}$.**

**Figure 11.** SERS spectrum and fingerprint of L-arginine. As told by Sherman et al., SERS spectra have previously been reported in the literature for this molecule [46],[47]. Let us add [48],[49].

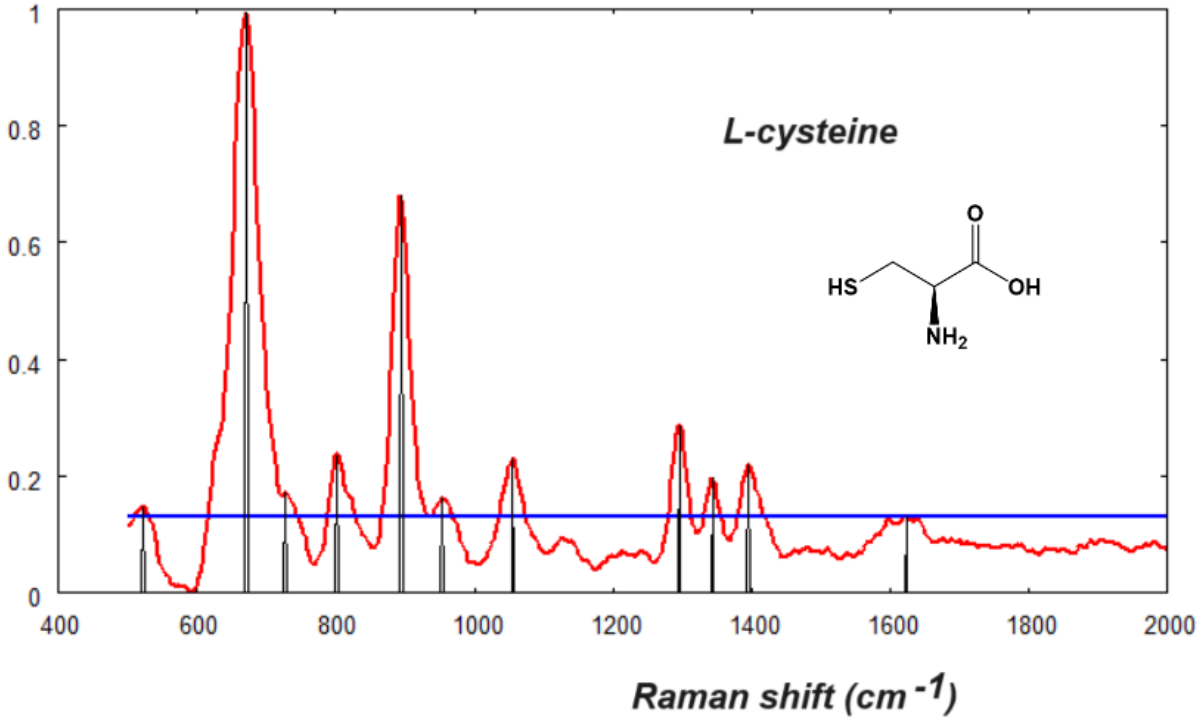


| Position (in cm -1) | Relative intensity | Position (in cm -1) | Relative intensity |
|---|---|---|---|
| 522.00 | 0.15 | 953.50 | 0.16 |
| 670.50 | 0.99 | 1055.50 | 0.23 |
| 727.00 | 0.17 | 1296.00 | 0.28 |
| 801.00 | 0.24 | 1344.00 | 0.20 |
| 894.00 | 0.68 | 1395.50 | 0.22 |
| | | 1623.50 | 0.13 |

**Main peak at 670.5 cm$^{-1}$.**

**Figure 12a.** SERS spectrum of L-cysteine. SERS spectra have previously been reported for this molecule [50],[51]. Let us add [52],[53],[54].

In the following Table II, we show the peaks as determined by means of the q-Gaussian deconvolution, proposed in [1]. We can observe some slight differences in the positions of the peak centers (differences are within the uncertainty of plus/minus 2 $cm^{-1}$). The other data considered are those form [50],[51],[53],[54].

| | | | | | | | | | | | | | |
|---|---|---|---|---|---|---|---|---|---|---|---|---|---|
| From Fig.12a | 522 | **670.5** | 727 | 801 | | **894** | 953.5 | | **1055. 5** | | | **1296** | **1344** | **1395.5** |
| Sherman et al., 2020. 631 | | 668.5 | 728.5 | 800 | 821 | 894 | 953 | | 1054 | 1121 | | 1295 | 1342 | 1397.5 |
| Diaz Fleming et al., 2009. | | 667 | 778 | 815 | | 903 | 947 | 1002 | 1058 | 1200 | | 1292 | 1347 | 1402 |
| Jing and Fang, 2007. | | 663 | 725 | | | 908 | | | 1033 | | | 1291 | 1341 | 1395 |
| Graff and Bukowska, 2005. | | 670 | 725 | | | 890 | | | | | | | | 1395 |
| Yao and Huang, 2018. | | 673 | 789 | | 832 | 900 | 949 | | 1050 | 1125 | 1232 | 1292 | 1339 | 1391 |

**Table II: SERS bands (positions in $cm^{-1}$) of L-Cysteine from literature here mentioned.**

Here in the following figure, an example of q-Gaussian fitting of L-cysteine.

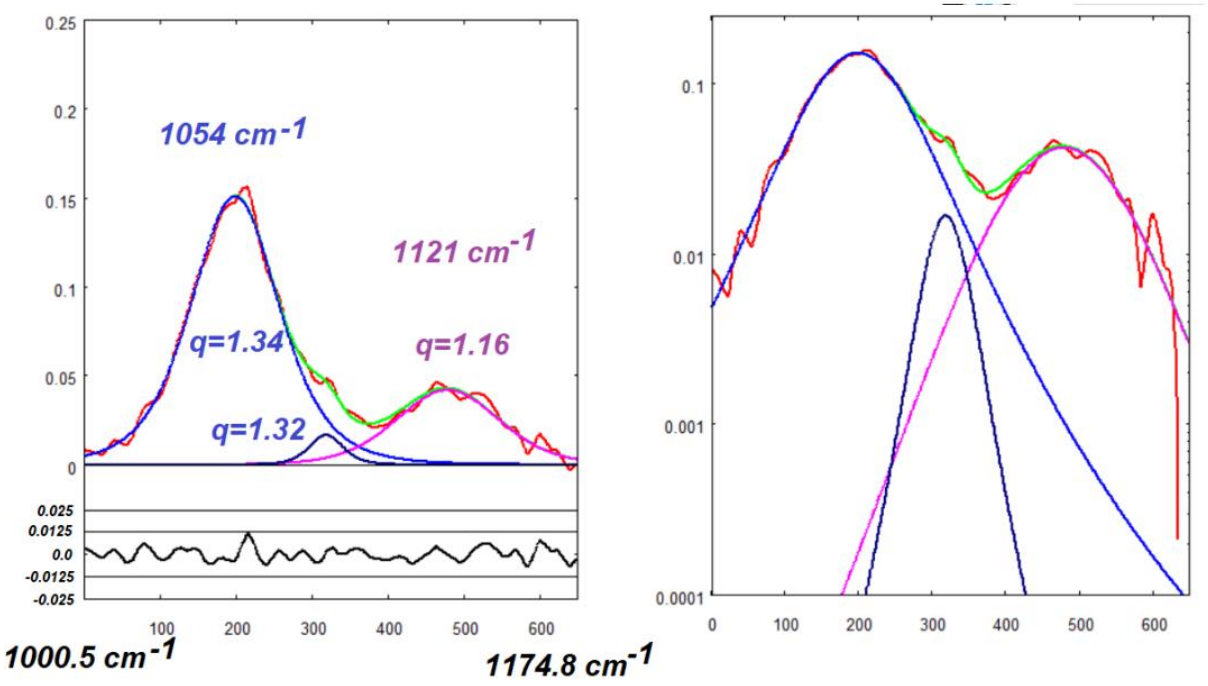


**Fig.12b.** The best fit (green) onto data (red) of L-Cysteine (Sherman et al., 2020) for the frequency range from 1000.5 to 1174.8 $cm^{-1}$. Three q-Gaussians have been used (values of the q-parameters are given in the figure). On the right, the same fit is shown with the log scale for y-axis (semi log scale).

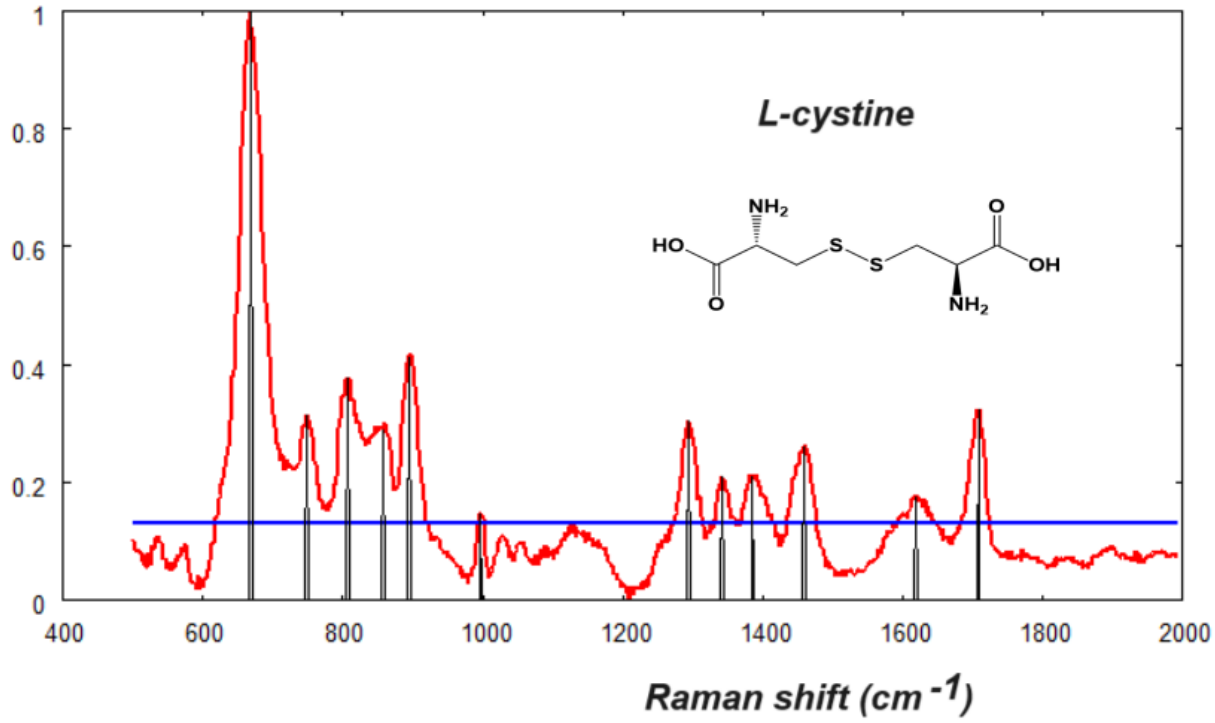


| Position (in cm -1) | Relative intensity | Position (in cm -1) | Relative intensity |
|---|---|---|---|
| 668.00 | 1.00 | 1294.50 | 0.30 |
| 748.50 | 0.31 | 1342.50 | 0.21 |
| 806.50 | 0.38 | 1386.00 | 0.21 |
| 857.50 | 0.29 | 1460.00 | 0.26 |
| 894.50 | 0.41 | 1619.50 | 0.17 |
| 997.00 | 0.15 | 1708.50 | 0.32 |

**Main peak at 668.0 cm$^{-1}$.**

**Figure 13.** SERS spectrum and fingerprint of L-cystine. Sherman et al. tell that SERS spectra have previously been reported for this molecule [55]. Let us add [56],[57].

As we did for homocysteine and homocysteine, let us compare the spectra.

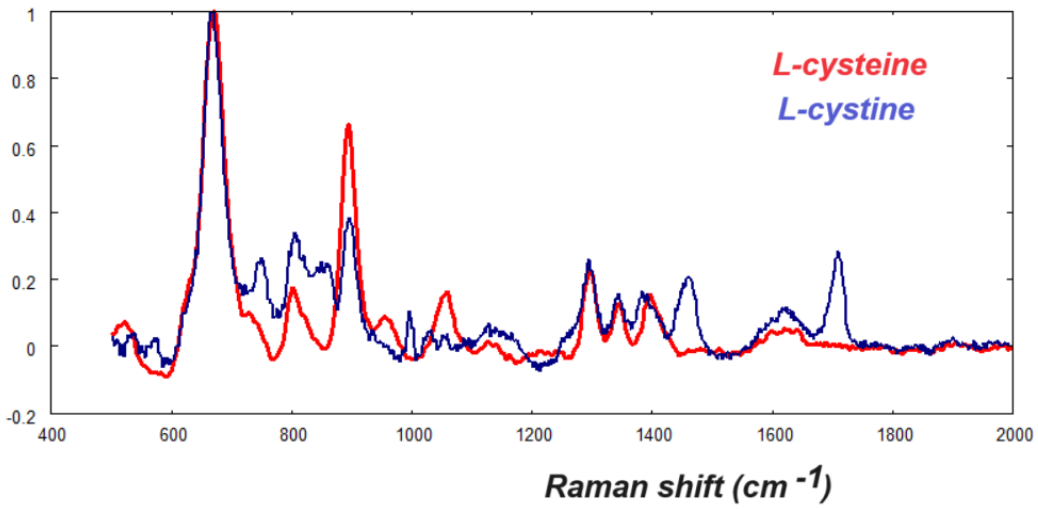


Comparing the fingerprints (within the uncertainty of plus/minus 2 $cm^{-1}$.):

| | | | | | | | | |
|---|---|---|---|---|---|---|---|---|
| L-cysteine | 522 | **670.5** | 727 | **801** | | **894** | 953.5 | 1055.5 |
| L-cystine | | **668** | 748.5 | **806.5** | 857.5 | **894.5** | 997 | |

| | | | | | | |
|---|---|---|---|---|---|---|
| L-cysteine | **1296** | **1344** | 1395.5 | | **1623.5** | |
| L-cystine | **1294.5** | **1342.5** | 1386 | 1460 | **1619.5** | 1708.5 |

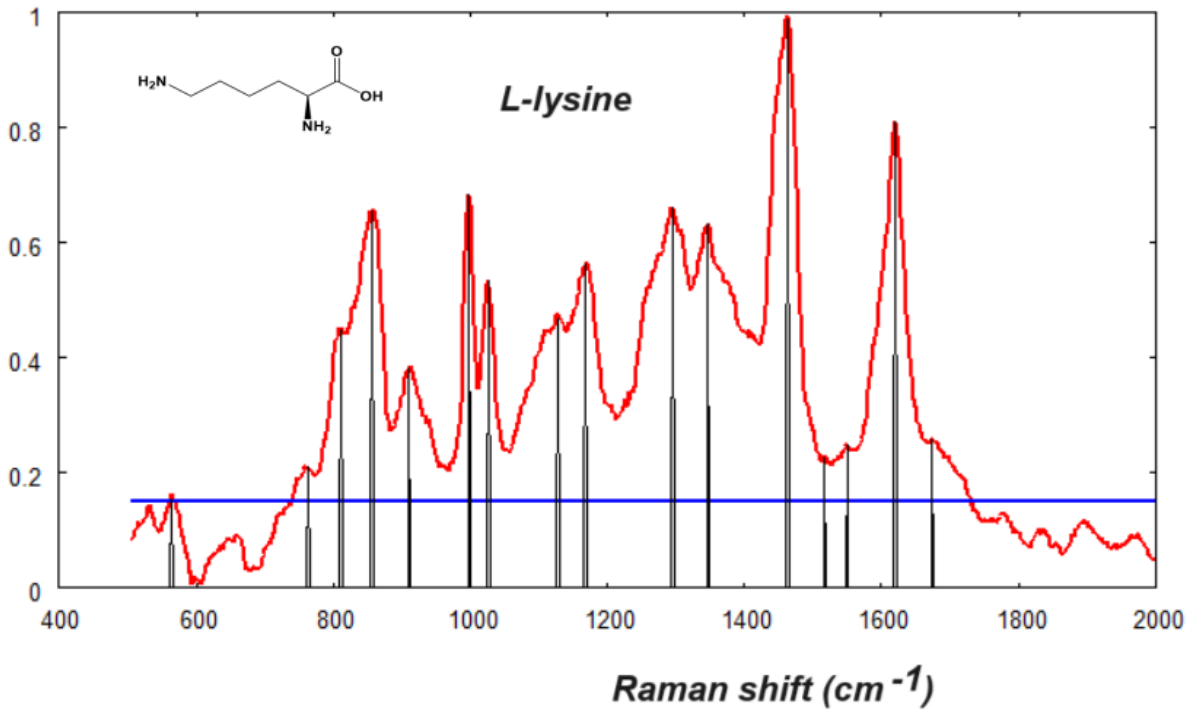


| Position (in cm -1) | Relative intensity | Position (in cm -1) | Relative intensity |
|---|---|---|---|
| 563.50 | 0.15 | 1168.00 | 0.56 |
| 762.50 | 0.21 | 1294.50 | 0.66 |
| 811.50 | 0.45 | 1347.00 | 0.63 |
| 855.50 | 0.66 | 1462.50 | 0.99 |
| 911.00 | 0.38 | 1517.50 | 0.23 |
| 998.00 | 0.68 | 1549.50 | 0.25 |
| 1026.50 | 0.53 | 1620.00 | 0.81 |
| 1127.50 | 0.47 | 1674.00 | 0.26 |

**Main peak at 1462.5 $cm^{-1}$.**

**Figure 14.** SERS spectrum of L-lysine. According to Sherman et al., SERS spectra have previously been reported for this molecule [58],[59]. Let us add [60],[61],[62].

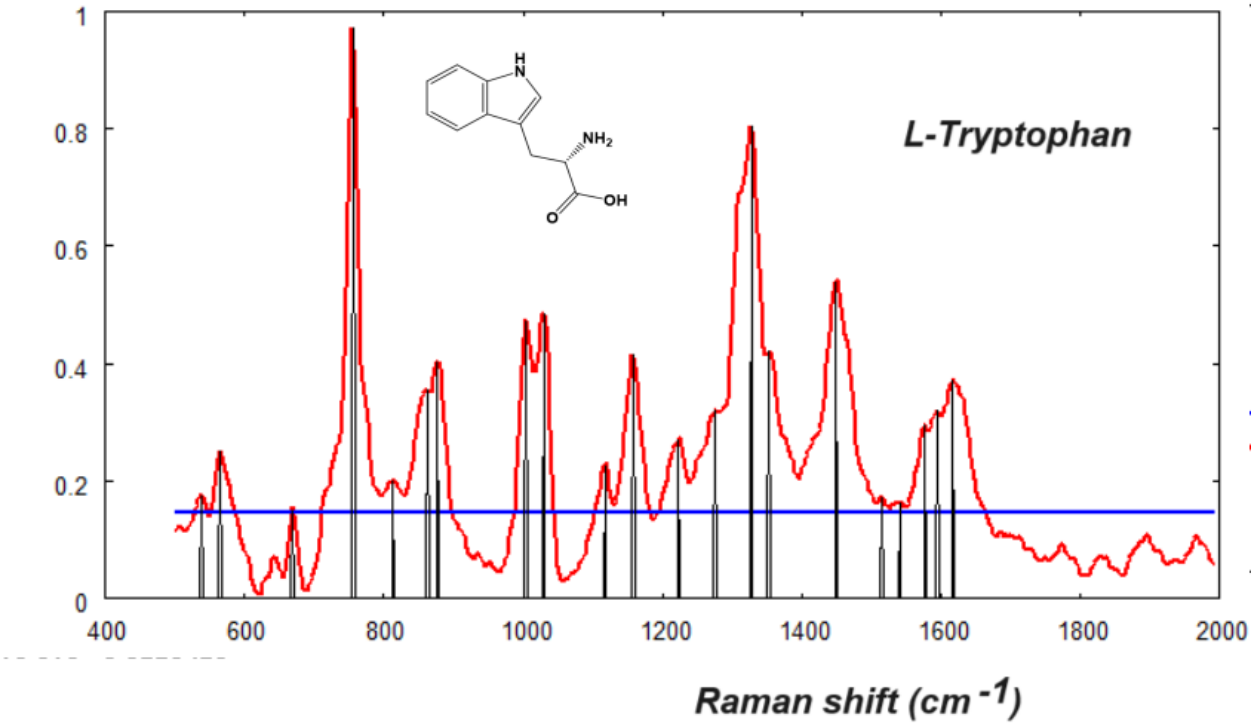


| Position (in cm -1) | Relative intensity | Position (in cm -1) | Relative intensity |
|---|---|---|---|
| 536.50 | 0.18 | 1223.50 | 0.27 |
| 564.00 | 0.25 | 1276.00 | 0.32 |
| 668.00 | 0.15 | 1328.00 | 0.80 |
| 755.50 | 0.97 | 1353.00 | 0.42 |
| 813.00 | 0.20 | 1449.50 | 0.54 |
| 861.50 | 0.35 | 1514.50 | 0.17 |
| 877.00 | 0.40 | 1541.00 | 0.16 |
| 1003.50 | 0.47 | 1577.00 | 0.30 |
| 1029.50 | 0.49 | 1595.50 | 0.32 |
| 1117.50 | 0.23 | 1617.50 | 0.37 |
| 1158.00 | 0.41 | | |

**Main peak at 755.5 $cm^{-1}$.**

**Figure 15.** SERS spectrum of L-tryptophan. Sherman et al. are mentioning the SERS spectra reported in [63],[64]. Let us add [60],[65],[66],[67].

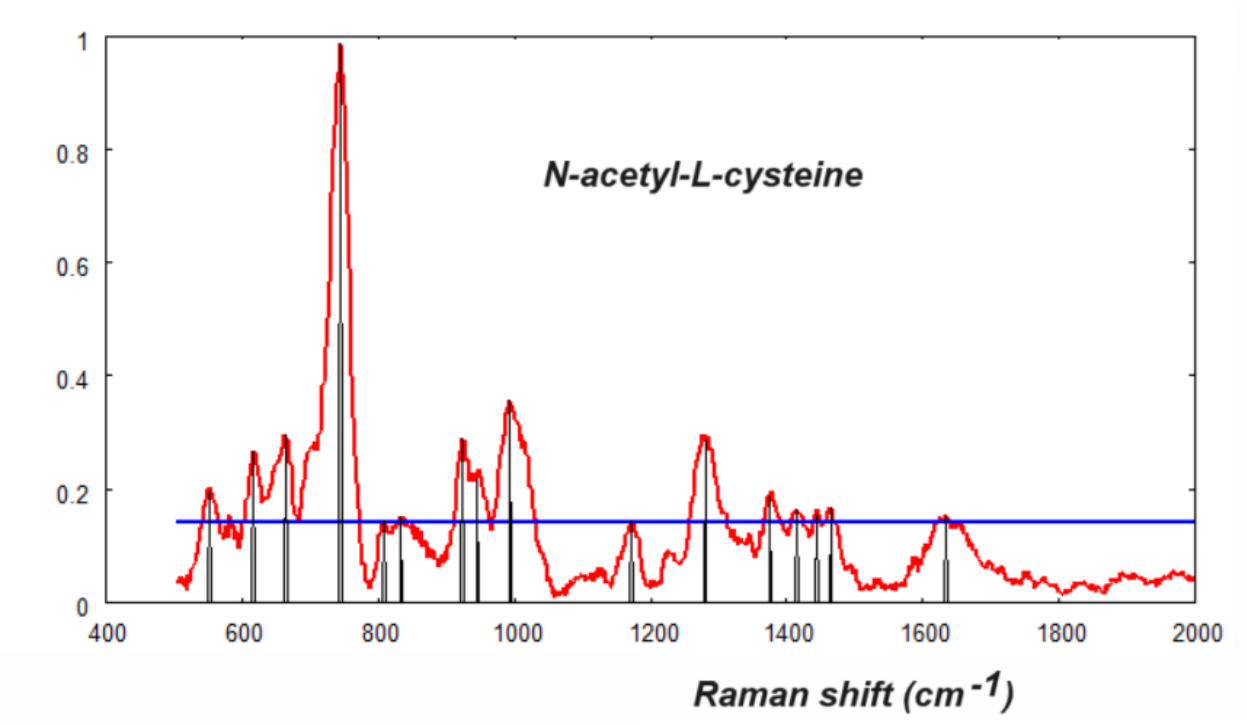


| Position (in cm$^{-1}$) | Relative intensity | Position (in cm$^{-1}$) | Relative intensity |
|---|---|---|---|
| 552.00 | 0.19 | 994.00 | 0.35 |
| 616.00 | 0.26 | 1172.5 | 0.14 |
| 663.50 | 0.29 | 1280.0 | 0.28 |
| 744.50 | 0.98 | 1376.0 | 0.18 |
| 809.00 | 0.14 | 1415.0 | 0.16 |
| 833.50 | 0.15 | 1444.0 | 0.15 |
| 924.00 | 0.28 | 1464.5 | 0.16 |
| 946.00 | 0.21 | 1634.0 | 0.15 |

**Main peak at 744.5 cm$^{-1}$.**

**Figure 16.** SERS spectrum and fingerprint of N-acetyl-L-cysteine. No reference provided by Sherman et al.

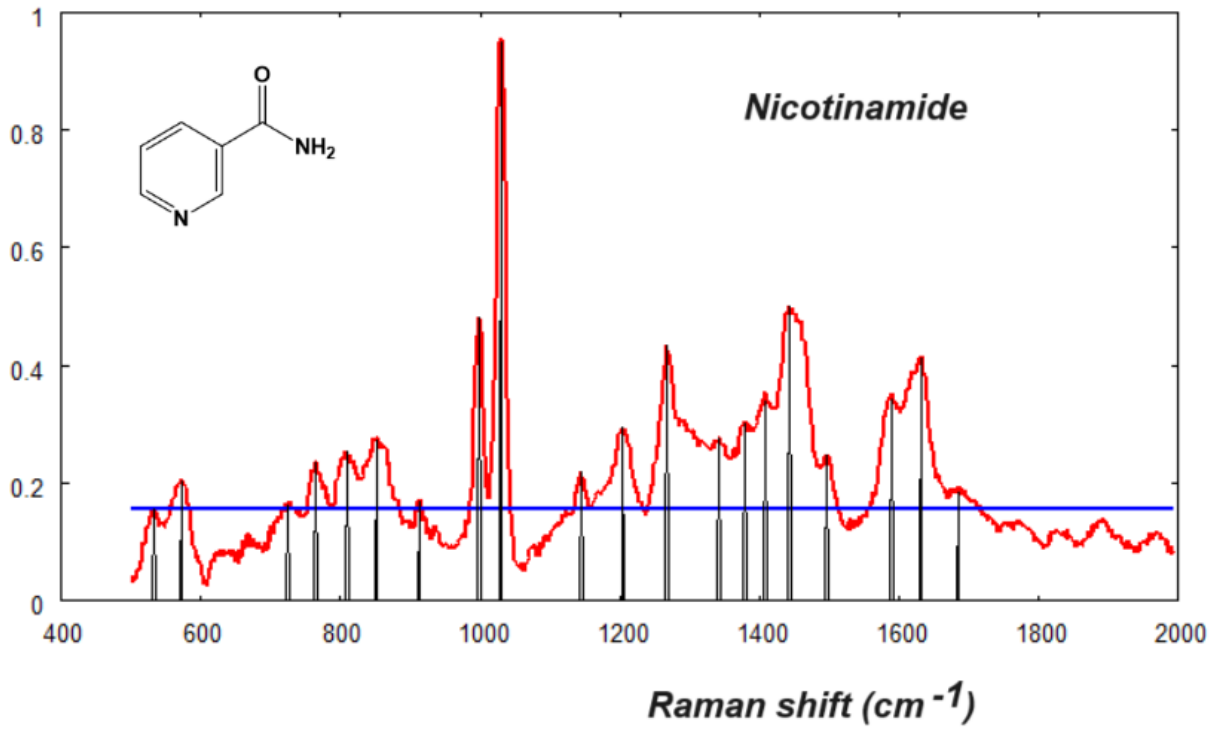


| Position (in cm$^{-1}$) | Relative intensity | Position (in cm$^{-1}$) | Relative intensity |
|---|---|---|---|
| 532.00 | 0.16 | 1204.50 | 0.29 |
| 571.00 | 0.20 | 1267.50 | 0.43 |
| 724.00 | 0.16 | 1342.50 | 0.28 |
| 764.50 | 0.24 | 1379.50 | 0.30 |
| 808.50 | 0.25 | 1408.50 | 0.34 |
| 850.50 | 0.27 | 1443.50 | 0.50 |
| 912.00 | 0.17 | 1496.50 | 0.25 |
| 999.00 | 0.48 | 1589.00 | 0.34 |
| 1029.50 | 0.95 | 1631.00 | 0.41 |
| 1145.00 | 0.22 | 1685.00 | 0.18 |

**Main peak at 1029.5 cm$^{-1}$.**

**Figure 17.** SERS spectrum and fingerprint of nicotinamide (Sherman et al. are reporting [68],[69],[70]). Let us add [71],[72].

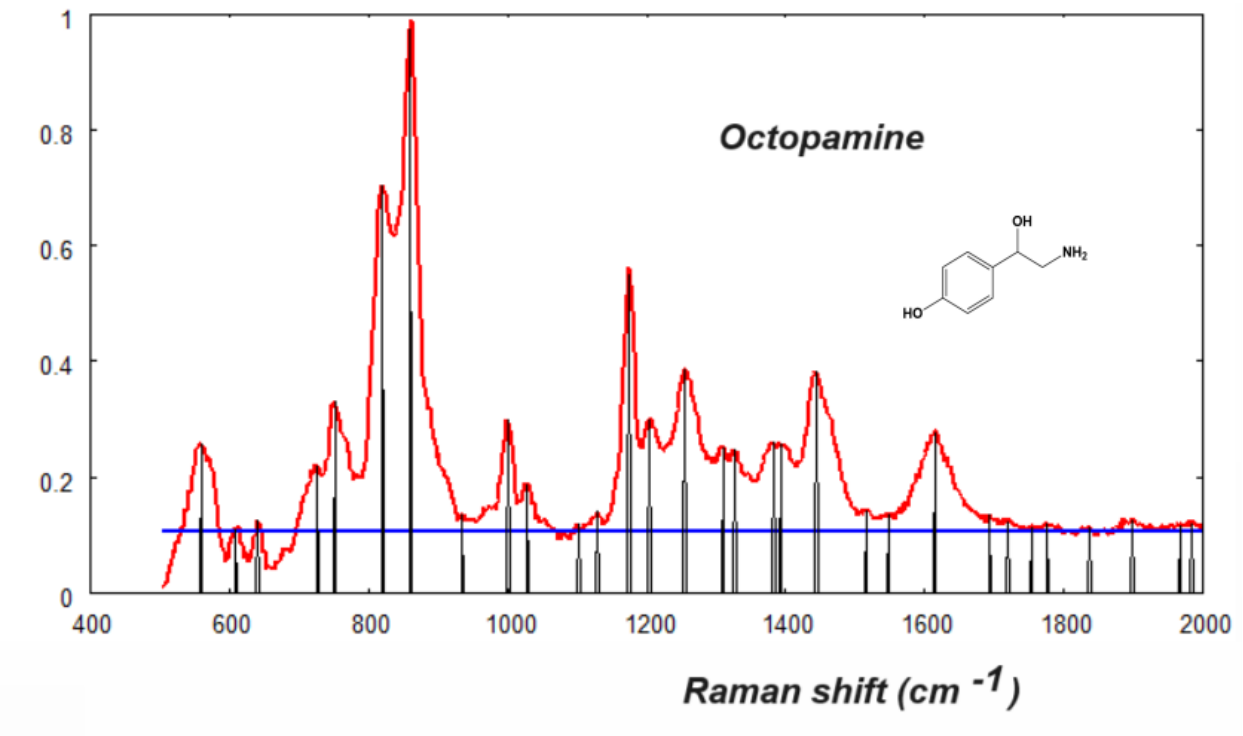


| Position (in cm$^{-1}$) | Relative intensity | Position (in cm$^{-1}$) | Relative intensity |
|---|---|---|---|
| 559.00 | 0.26 | 1326.00 | 0.25 |
| 609.00 | 0.11 | 1382.00 | 0.26 |
| 640.50 | 0.12 | 1392.50 | 0.26 |
| 726.50 | 0.22 | 1444.00 | 0.38 |
| 751.00 | 0.33 | 1515.00 | 0.14 |
| 820.00 | 0.70 | 1547.50 | 0.14 |
| 860.00 | 0.97 | 1614.00 | 0.28 |
| 935.00 | 0.13 | 1693.50 | 0.13 |
| 1000.50 | 0.30 | 1719.50 | 0.12 |
| 1028.50 | 0.19 | 1753.00 | 0.11 |
| 1102.00 | 0.12 | 1776.50 | 0.12 |
| 1129.50 | 0.14 | 1836.50 | 0.11 |
| 1174.50 | 0.55 | 1898.50 | 0.12 |
| 1204.00 | 0.30 | 1967.00 | 0.12 |
| 1255.00 | 0.39 | 1984.00 | 0.12 |
| 1309.50 | 0.25 | | |

**Main peak at 860.0 cm$^{-1}$.**

**Figure 18.** SERS spectrum and fingerprint of octopamine. SERS spectra previously reported, mentioned by Sherman et al., are available in [73].

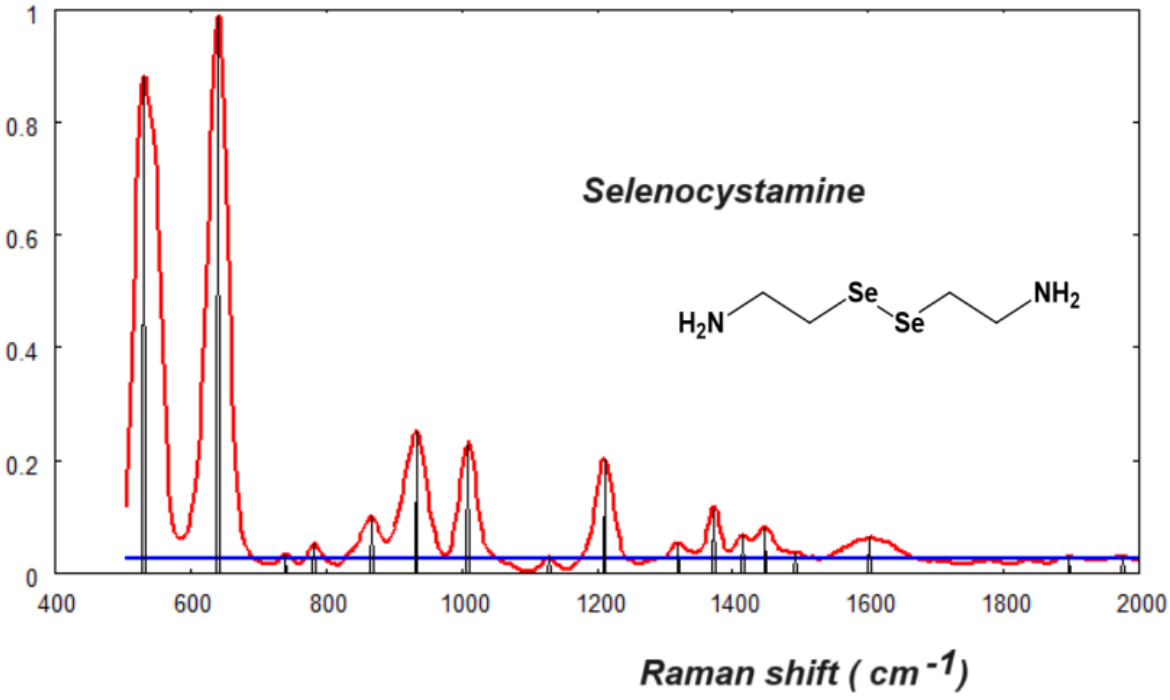


| Position (in cm -1) | Relative intensity | Position (in cm -1) | Relative intensity |
|---|---|---|---|
| 531.50 | 0.88 | 1319.50 | 0.05 |
| 640.50 | 0.99 | 1371.50 | 0.12 |
| 740.00 | 0.03 | 1415.00 | 0.07 |
| 782.50 | 0.05 | 1448.00 | 0.08 |
| 866.50 | 0.10 | 1493.00 | 0.04 |
| 932.50 | 0.25 | 1602.00 | 0.06 |
| 1009.00 | 0.23 | 1896.50 | 0.03 |
| 1129.50 | 0.03 | 1976.50 | 0.03 |
| 1210.50 | 0.20 | | |

**Main peak at 640.5 $cm^{-1}$.**

**Figure 19.** SERS spectrum and fingerprint of selenocystamine. No reference provided by Sherman et al.

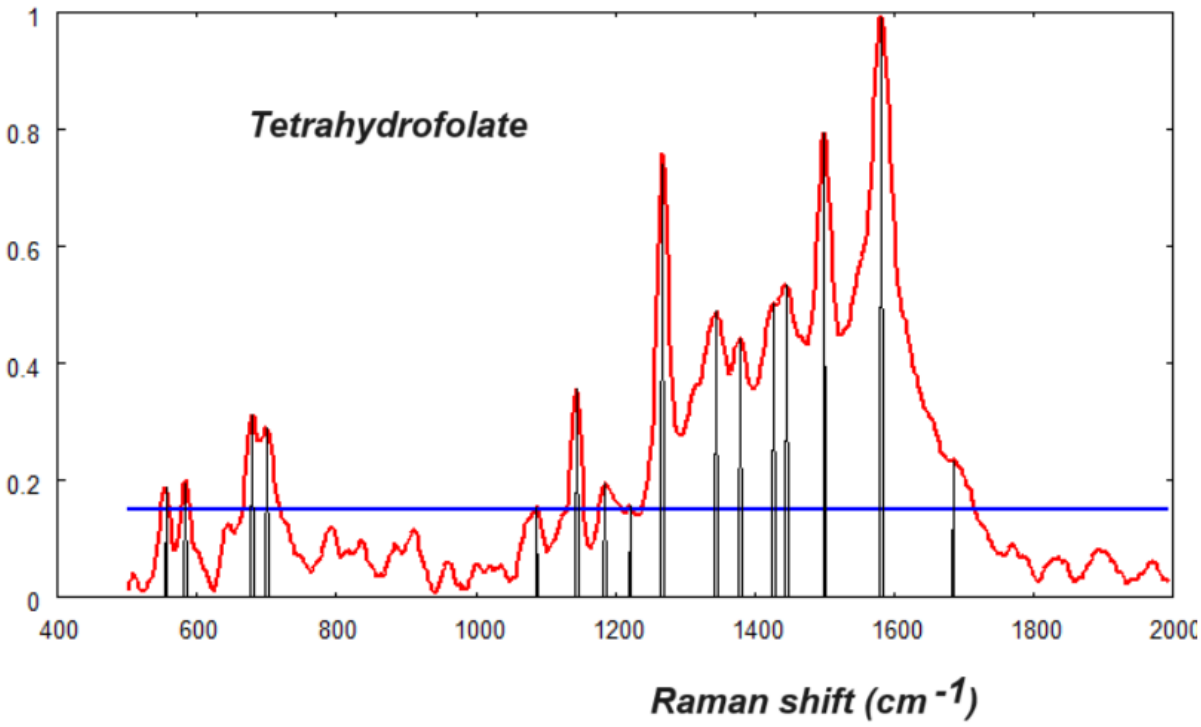


| Position (in cm -1) | Relative intensity | Position (in cm -1) | Relative intensity |
|---|---|---|---|
| 555.000 | 0.18 | 1267.50 | 0.73 |
| 582.000 | 0.19 | 1344.50 | 0.48 |
| 679.500 | 0.31 | 1379.50 | 0.44 |
| 699.500 | 0.28 | 1427.00 | 0.50 |
| 1087.50 | 0.15 | 1445.50 | 0.53 |
| 1145.00 | 0.35 | 1500.50 | 0.79 |
| 1185.50 | 0.19 | 1581.00 | 0.99 |
| 1221.50 | 0.15 | 1685.00 | 0.23 |

**Main peak at 1581.0 $cm^{-1}$.**

**Figure 20.** SERS spectrum of tetrahydrofolate. No reference mentioned by Sherman et al.

In the following plot, the SERS spectra of dihydrofolate and tetrahydrofolate are shown together.

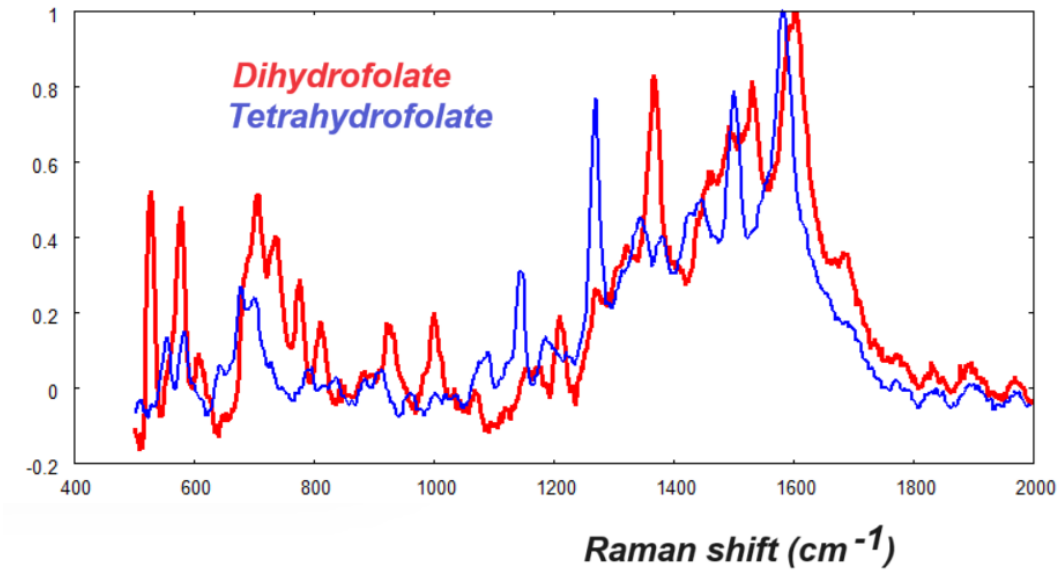

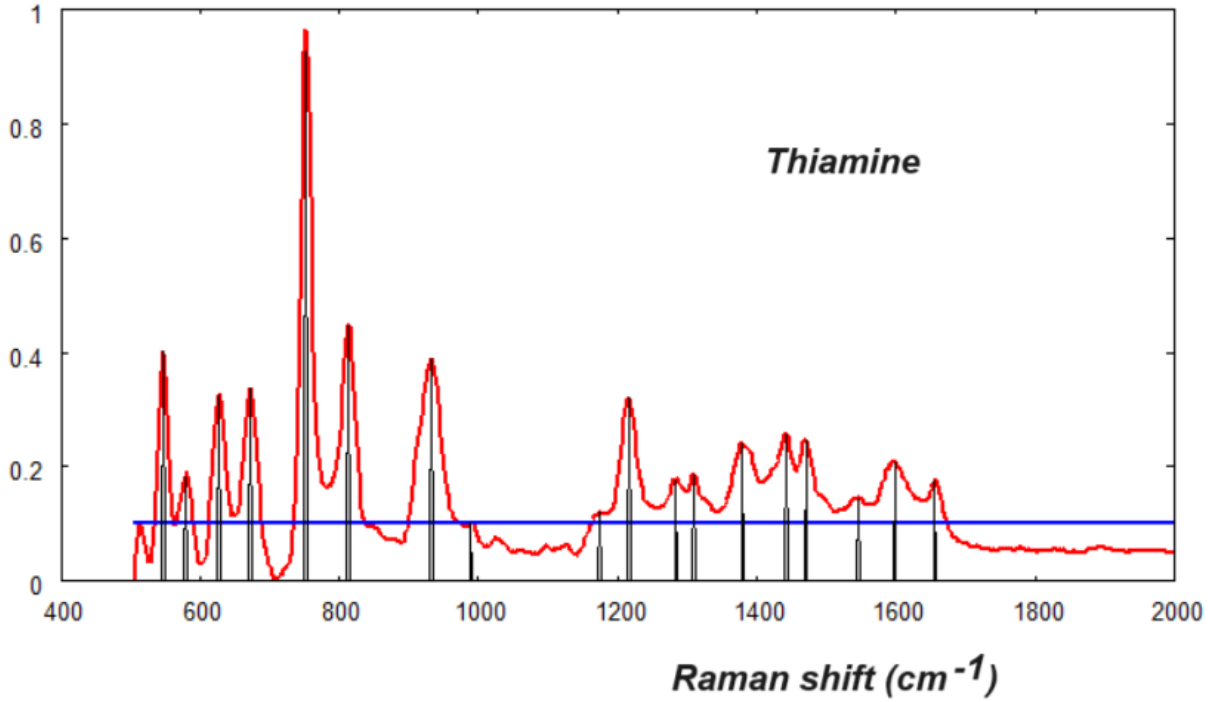


| Position (in cm$^{-1}$) | Relative intensity | Position (in cm$^{-1}$) | Relative intensity |
|---|---|---|---|
| 547.50 | 0.40 | 1217.00 | 0.32 |
| 579.50 | 0.18 | 1284.00 | 0.18 |
| 627.00 | 0.33 | 1309.50 | 0.18 |
| 672.50 | 0.34 | 1380.00 | 0.24 |
| 751.00 | 0.93 | 1442.00 | 0.26 |
| 813.50 | 0.45 | 1470.50 | 0.25 |
| 932.50 | 0.39 | 1545.50 | 0.14 |
| 989.50 | 0.10 | 1598.00 | 0.21 |
| 1174.50 | 0.12 | 1656.00 | 0.18 |

**Main peak at 751.0 cm$^{-1}$.**

**Figure 21.** SERS spectrum and fingerprint of thiamine. SERS spectra have been previously reported for this molecule [74], according to Sherman et al.

**Discussion**

In this research we have proposed the fingerprints of some SERS (Surface-Enhanced Raman) spectra of metabolites, provided by Sherman et al. in 2020. For Cysteamine and L-Cysteine, we have proposed comparison with other data from literature. Very interesting are the SERS fingerprints from Sherman et al. data of Homocysteine, Homocystine, L-cysteine and L-cystine. Due to the remarkable quality of spectra, we can easily identify the common SERS bands. Let us repeat here the comparison (fingerprints are given in $cm^{-1}$.)

Comparisons (within the uncertainty of plus/minus 2 $cm^{-1}$.):

a) Fingerprints of Homocysteine and Homocystine:

| | | | | | | | | | | | | | | | |
|---|---|---|---|---|---|---|---|---|---|---|---|---|---|---|---|
| Homocysteine | | | 643 | **708.5** | **764.5** | | | | **893** | 976.5 | 1011 | | | | |
| Homocystine | 524.5 | 638.5 | **708.5** | **762.5** | 811.5 | 871 | **891** | | 998 | 1020 | | | | | |
| Homocysteine | **1052.5** | | | | **1269.5** | **1328** | **1347** | **1421** | 1476.5 | 1493 | 1545.5 | | **1632** | **1711.5** | |
| Homocystine | **1052.5** | 1129.5 | 1149 | **1267.5** | **1330** | **1344.5** | **1419** | 1460 | | | 1620 | | **1634** | **1715.5** | |

b) Fingerprints of L-cysteine and L-cystine:

| | | | | | | | | | |
|---|---|---|---|---|---|---|---|---|---|
| L-cysteine | 522 | **670.5** | 727 | **801** | | **894** | 953.5 | 1055.5 | |
| L-cystine | | **668** | 748.5 | **806.5** | 857.5 | **894.5** | 997 | | |
| L-cysteine | **1296** | **1344** | 1395.5 | | | **1623.5** | | | |
| L-cystine | **1294.5** | **1342.5** | 1386 | 1460 | | **1619.5** | 1708.5 | | |

c) Fingerprints of Homocystine and L-cystine:

| | | | | | | | | | | | | |
|---|---|---|---|---|---|---|---|---|---|---|---|---|
| Homocystine | 524.5 | 638.5 | 708.5 | 762.5 | 811.5 | 871 | **891** | **998** | 1020 | 1052.5 | 1129.5 | 1149 |
| L-cystine | | | 668 | 748.5 | 806.5 | 857.5 | **894.5** | **997** | | | | |
| Homocystine | 1267.5 | 1330 | **1344.5** | 1419 | **1460** | | **1620** | 1634 | 1715.5 | | | |
| L-cystine | 1294.5 | | **1342.5** | 1386 | **1460** | | **1619.5** | 1708.5 | | | | |

d) Fingerprints of Homocysteine and L-cysteine:

| | | | | | | | | | | | |
|---|---|---|---|---|---|---|---|---|---|---|---|
| Homocysteine | | 643 | 708.5 | 764.5 | **893** | 976.5 | 1011 | **1052.5** | | | |
| L-cysteine | 522 | 670.5 | 727 | 801 | **894** | 953.5 | | **1055.5** | | | |
| Homocysteine | 1269.5 | 1328 | **1347** | 1421 | 1476.5 | 1493 | 1545.5 | 1632 | 1711.5 | | |
| L-cysteine | 1296 | | **1344** | 1395.5 | | | 1623.5 | | | | |

Therefore, a proper strategy for identifying the SERS bands is that of using comparisons of several of them. For instance, the four metabolites here considered have common bands at 891-894.5 $cm^{-1}$ and 1342.5-1347 $cm^{-1}$.

**References**

[1] Sparavigna, A. C. (2023). SERS Spectral Bands of L-Cysteine, Cysteamine and Homocysteine Fitted by Tsallis q-Gaussian Functions. International Journal of Sciences, 12(09), 14-24.
[2] Sherman, L. M., Petrov, A. P., Karger, L. F., Tetrick, M. G., Dovichi, N. J., & Camden, J. P. (2020). A surface-enhanced Raman spectroscopy database of 63 metabolites. Talanta, 210, 120645.
[3] Sparavigna, A. C. (2023). q-Gaussian Tsallis Line Shapes and Raman Spectral Bands. International Journal of Sciences, 12(03), 27-40.
[4] Sparavigna, A. C. (2023). q-Gaussian Tsallis Functions and Egelstaff-Schofield Spectral Line Shapes. International Journal of Sciences, 12(03), 47-50.
[5] Sparavigna, A. C. (2023). q-Gaussian Tsallis Line Shapes for Raman Spectroscopy (June 7, 2023). SSRN Electronic Journal. DOI: 10.2139/ssrn.4445044
[6] Sparavigna, A. C. (2023). Formamide Raman Spectrum and qGaussian Tsallis Lines (June 12, 2023). SSRN Electronic Journal. DOI: 10.2139/ssrn.4451881
[7] Sparavigna A. C. (2023). Tsallis q-Gaussian function as fitting lineshape for Graphite Raman bands. ChemRxiv. Cambridge: Cambridge Open Engage; 2023.
[8] Sparavigna, A. C. (2023). Generalizing asymmetric and pseudo-Voigt functions by means of q-Gaussian Tsallis functions to analyze the wings of Raman spectral bands. ChemRxiv. Cambridge: Cambridge Open Engage; 2023.
[9] Fenske, M. R., Braun, W. G., Wiegand, R. V., Quiggle, D., McCormick, R., & Rank, D. H. (1947). Raman spectra of hydrocarbons. Analytical Chemistry, 19(10), 700-765.
[10] D'Ippolito, V., Andreozzi, G. B., Bersani, D., & Lottici, P. P. (2015). Raman fingerprint of chromate, aluminate and ferrite spinels. Journal of Raman Spectroscopy, 46(12), 1255-1264.
[11] Sparavigna, A. C. (2023). The Raman Fingerprints of Quartz, Albite and Calcite. Submitted SSRN
[12] Mosier-Boss, P. A., Lieberman, S. H., & Newbery, R. (1995). Fluorescence rejection in Raman spectroscopy by shifted-spectra, edge detection, and FFT filtering techniques. Applied Spectroscopy, 49(5), 630-638.
[13] Dongil, A. B., Bachiller-Baeza, B., Rodríguez-Ramos, I., & Guerrero-Ruiz, A. (2014). Exploring the insertion of ethylenediamine and bis (3-aminopropyl) amine into graphite oxide. Nanoscience Methods, 3(1), 28-39.
[14] I. Pavel, A. Szeghalmi, D. Moigno, S. Cîntă, W. Kiefer, Theoretical and pH dependent surface enhanced Raman spectroscopy study on caffeine, Biopolymers 72(1) (2003) 25-37.
[15] O. Alharbi, Y. Xu, R. Goodacre, Simultaneous multiplexed quantification of caffeine and its major metabolites theobromine and paraxanthine using surface-enhanced Raman scattering, Analytical and Bioanalytical Chemistry 407(27) (2015) 8253-8261.
[16] H. Zheng, D. Ni, Z. Yu, P. Liang, H. Chen, Fabrication of flower-like silver nanostructures for rapid detection of caffeine using surface enhanced Raman spectroscopy, Sensors and Actuators B: Chemical 231 (2016) 423-430.
[17] Hédoux, A., Decroix, A. A., Guinet, Y., Paccou, L., Derollez, P., & Descamps, M. (2011). Low-and high-frequency Raman investigations on caffeine: polymorphism, disorder and phase transformation. The Journal of Physical Chemistry B, 115(19), 5746-5753.
[18] Baranska, M., & Proniewicz, L. M. (2008). Raman mapping of caffeine alkaloid. Vibrational Spectroscopy, 48(1), 153-157.

[19] Kang, J., Gu, H., Zhong, L., Hu, Y., & Liu, F. (2011). The pH dependent Raman spectroscopic study of caffeine. Spectrochimica Acta Part A: Molecular and Biomolecular Spectroscopy, 78(2), 757-762.
[20] Edwards, H. G., Munshi, T., & Anstis, M. (2005). Raman spectroscopic characterisations and analytical discrimination between caffeine and demethylated analogues of pharmaceutical relevance. Spectrochimica Acta Part A: Molecular and Biomolecular Spectroscopy, 61(7), 1453-1459.
[21] Zareef, M., Hassan, M. M., Arslan, M., Ahmad, W., Ali, S., Ouyang, Q., Li, H., Wu, X. & Chen, Q. (2020). Rapid prediction of caffeine in tea based on surface-enhanced Raman spectroscopy coupled multivariate calibration. Microchemical Journal, 159, 105431.
[22] O. Dong, D.C.C. Lam, Silver nanoparticles as surface-enhanced Raman substrate for quantitative identification of label-free proteins, Materials Chemistry and Physics 126(1) (2011) 91-96.
[23] Podstawka, E., Ozaki, Y., & Proniewicz, L. M. (2004). Part I: Surface-enhanced Raman spectroscopy investigation of amino acids and their homodipeptides adsorbed on colloidal silver. Applied spectroscopy, 58(5), 570-580.
[24] A. Michota, A. Kudelski, J. Bukowska, Influence of electrolytes on the structure of cysteamine monolayer on silver studied by surface-enhanced Raman scattering, Journal of Raman Spectroscopy 32(5) (2001) 345-350.
[25] A. Michota, A. Kudelski, J. Bukowska, Chemisorption of Cysteamine on Silver Studied by Surface-Enhanced Raman Scattering, Langmuir 16(26) (2000) 10236-10242.
[26] T. Goto, H. Watarai, SERS Study of Rotational Isomerization of Cysteamine Induced by Magnetic Pulling Force, Langmuir 26(7) (2010) 4848-4853.
[27] A. Michota, A. Kudelski, J. Bukowska, Molecular structure of cysteamine monolayers on silver and gold substrates: Comparative studies by surface-enhanced Raman scattering, Surface Science 502-503 (2002) 214-218.
[28] X. Jiang, M. Yang, Y. Meng, W. Jiang, J. Zhan, Cysteamine-Modified Silver Nanoparticle Aggregates for Quantitative SERS Sensing of Pentachlorophenol with a Portable Raman Spectrometer, ACS Applied Materials & Interfaces 5(15) (2013) 6902-6908.
[29] Kudelski, A., & Hill, W. (1999). Raman study on the structure of cysteamine monolayers on silver. Langmuir, 15(9), 3162-3168.
[30] I. Delfino, A.R. Bizzarri, S. Cannistraro, Single-molecule detection of yeast cytochrome c by Surface-Enhanced Raman Spectroscopy, Biophysical Chemistry 113(1) (2005) 41-51.
[31] L.-L. Qu, D.-W. Li, L.-X. Qin, J. Mu, J.S. Fossey, Y.-T. Long, Selective and Sensitive Detection of Intracellular O2•– Using Au NPs/Cytochrome c as SERS Nanosensors, Analytical Chemistry 85(20) (2013) 9549-9555.
[32] Strekas, T. C., & Spiro, T. G. (1972). Cytochrome c: resonance Raman spectra. Biochimica et Biophysica Acta (BBA)-Protein Structure, 278(1), 188-192.
[33] Murgida, D. H., & Hildebrandt, P. (2004). Electron-transfer processes of cytochrome c at interfaces. New insights by surface-enhanced resonance Raman spectroscopy. Accounts of chemical research, 37(11), 854-861.
[34] Brazhe, N. A., Evlyukhin, A. B., Goodilin, E. A., Semenova, A. A., Novikov, S. M., Bozhevolnyi, S. I., Chichkov, B. N., Sarycheva, A. S., Baizhumanov, A. A., Nikelshparg, E. I., Deev, L. I., Maksimov, E. G., Maksimov, G. V. & Sosnovtseva, O. (2015). Probing cytochrome c in living mitochondria with surface-enhanced Raman spectroscopy. Scientific reports, 5(1), 13793.

[35] F. Gao, E. Grant, X. Lu, Determination of histamine in canned tuna by molecularly imprinted polymers-surface enhanced Raman spectroscopy, Analytica Chimica Acta 901 (2015) 68-75.
[36] W.-C. Lin, T.-R. Tsai, H.-L. Huang, C.Y. Shiau, H.-P. Chiang, SERS Study of Histamine by Using Silver Film over Nanosphere Structure, Plasmonics 7(4) (2012) 709-716.
[37] T. Janči, D. Valinger, J. Gajdoš Kljusurić, L. Mikac, S. Vidaček, M. Ivanda, Determination of histamine in fish by Surface Enhanced Raman Spectroscopy using silver colloid SERS substrates, Food Chemistry 224 (2017) 48-54.
[38] Chen, C., Zhang, Y., Wang, X., Qiao, X., Waterhouse, G. I., & Xu, Z. (2024). A core-satellite self-assembled SERS aptasensor containing a "biological-silent region" Raman tag for the accurate and ultrasensitive detection of histamine. Food Science and Human Wellness, 13(2), 1029-1039.
[39] Chen, C., Wang, X., Waterhouse, G. I., Qiao, X., & Xu, Z. (2022). A surface-imprinted surface-enhanced Raman scattering sensor for histamine detection based on dual semiconductors and Ag nanoparticles. Food Chemistry, 369, 130971.
[40] Torreggiani, A., Tamba, M., Bonora, S., & Fini, G. (2003). Raman and IR study on copper binding of histamine. Biopolymers: Original Research on Biomolecules, 72(4), 290-298.
[41] Itabashi, M., Shoji, K., & Itoh, K. (1982). Raman spectra of copper (II)-histamine (1: 2) and nickel (II)-histamine (1: 2) aqueous solutions. Inorganic Chemistry, 21(9), 3484-3489.
[42] Zheng, X. B., Liu, S. H., Panneerselvam, R., Zhang, Y. J., Wang, A., Zhang, F. L., Jin, S., & Li, J. F. (2023). Clinical detection of total homocysteine in human serum using surface-enhanced Raman spectroscopy. Vibrational Spectroscopy, 126, 103526.
[43] S. Nie, C.G. Castillo, K.L. Bergbauer, J.F.R. Kuck, I.R. Nabiev, N.-T. Yu, Surface-Enhanced Raman Spectra of Eye Lens Pigments, Applied Spectroscopy 44(4) (1990) 571-575.
[44] Das, G. M., Managò, S., Mangini, M., & De Luca, A. C. (2021). Biosensing using SERS active gold nanostructures. Nanomaterials, 11(10), 2679.
[45] Plou, J., García, I., Charconnet, M., Astobiza, I., García-Astrain, C., Matricardi, C., Mihi, A.; Carracedo, A., & Liz-Marzán, L.M. (2020). Multiplex SERS detection of metabolic alterations in tumor extracellular media. Adv. Funct. Mater. 2020, 30, 1910335.
[46] A.E. Aliaga, C. Garrido, P. Leyton, G. Diaz F, J.S. Gomez-Jeria, T. Aguayo, E. Clavijo, M.M. Campos-Vallette, S. Sanchez-Cortes, SERS and theoretical studies of arginine, Spectrochimica Acta Part A: Molecular and Biomolecular Spectroscopy 76(5) (2010) 458-463.
[47] C. Garrido, T. Aguayo, E. Clavijo, J.S. Gómez-Jeria, M.M. Campos-Vallette, The effect of the pH on the interaction of L-arginine with colloidal silver nanoparticles. A Raman and SERS study, Journal of Raman Spectroscopy 44(8) (2013) 1105-1110.
[48] Botta, R., & Bansal, C. (2015, June). Surface enhanced Raman scattering (SERS) study of L-arginine adsorbed on Ag nanoclusters on glass substrate by nanocluster deposition method. In AIP Conference Proceedings (Vol. 1665, No. 1). AIP Publishing.
[49] Dummitt, R. (2023). Chemical Effects in Protein Analysis: A Systematic Investigation of Amino Acid Spontaneous Raman and SERS Responses (Doctoral dissertation, The Ohio State University).
[50] G. Diaz Fleming, J.J. Finnerty, M. Campos-Vallette, F. Célis, A.E. Aliaga, C. Fredes, R. Koch, Experimental and theoretical Raman and surface-enhanced Raman scattering study of cysteine, Journal of Raman Spectroscopy 40(6) (2009) 632-638.
[51] C. Jing, Y. Fang, Experimental (SERS) and theoretical (DFT) studies on the adsorption behaviors of l-cysteine on gold/silver nanoparticles, Chemical Physics 332(1) (2007) 27-32.
[52] Brolo, A. G., Germain, P., & Hager, G. (2002). Investigation of the adsorption of L-cysteine on a polycrystalline silver electrode by surface-enhanced Raman scattering (SERS) and surface-

enhanced second harmonic generation (SESHG). The Journal of Physical Chemistry B, 106(23), 5982-5987.
[53] Graff, M., & Bukowska, J. (2005). Adsorption of Enantiomeric and Racemic Cysteine on a Silver Electrode− SERS Sensitivity to Chirality of Adsorbed Molecules. The Journal of Physical Chemistry B, 109(19), 9567-9574.
[54] Yao, G., & Huang, Q. (2018). DFT and SERS Study of l-Cysteine Adsorption on the Surface of Gold Nanoparticles. The Journal of Physical Chemistry C, 122(27), 15241-15251.
[55] H. Lee, M.S. Kim, S.W. Suh, Raman spectroscopy of sulphur-containing amino acids and their derivatives adsorbed on silver, Journal of Raman Spectroscopy 22(2) (1991) 91-96.
[56] Su, Y., Hessou, E. P., Colombo, E., Belletti, G., Moussadik, A., Lucas, I. T., Frochot, V., Daudon, M., Rouzière, S., Bazin, D., Li, K., Quaino, P. & Tielens, F. (2022). Crystalline structures of l-cysteine and l-cystine: a combined theoretical and experimental characterization. Amino Acids, 54(8), 1123-1133.
[57] Itoh, N., & Hanari, N. (2022). Reliable estimation of Raman shifts for peaks of l-cystine (NMIJ CRM 6025-a) in the low-frequency region. Analytical Sciences, 38(4), 657-664.
[58] A. Sengupta, M.L. Laucks, N. Dildine, E. Drapala, E.J. Davis, Bioaerosol characterization by surface-enhanced Raman spectroscopy (SERS), Journal of Aerosol Science 36(5) (2005) 651-664.
[59] A.E. Aliaga, I. Osorio-Roman, C. Garrido, P. Leyton, J. Cárcamo, E. Clavijo, J.S. Gómez-Jeria, G.D. F, M.M. Campos-Vallette, Surface enhanced Raman scattering study of l-lysine, Vibrational Spectroscopy 50(1) (2009) 131-135.
[60] Aboltaman, R., Kiamehr, Z., Cheraghi, A., & Malekfar, R. (2023). Application of sensitive SERS plasmonic biosensor for high detection of metabolic disorders. Spectrochimica Acta Part A: Molecular and Biomolecular Spectroscopy, 290, 122204.
[61] Yao, G., & Huang, Q. (2022). Theoretical and experimental study of the infrared and Raman spectra of L-lysine acetylation. Spectrochimica Acta Part A: Molecular and Biomolecular Spectroscopy, 278, 121371.
[62] Das, S., Satpati, B., Bhattacharya, T. S., & Bala, T. (2020). Synthesis of Au–Ag triangular nanocomposite with promising SERS activity. Nano-Structures & Nano-Objects, 22, 100438.
[63] A.E. Aliaga, I. Osorio-Román, P. Leyton, C. Garrido, J. Cárcamo, C. Caniulef, F. Célis, G. Díaz F., E. Clavijo, J.S. Gómez-Jeria, M.M. Campos-Vallette, Surface-enhanced Raman scattering study of L-tryptophan, Journal of Raman Spectroscopy 40(2) (2009) 164-169.
[64] L.-L. Qu, D.-W. Li, J.-Q. Xue, W.-L. Zhai, J.S. Fossey, Y.-T. Long, Batch fabrication of disposable screen printed SERS arrays, Lab on a Chip 12(5) (2012) 876-881.
[65] Gao, W., Duan, W., Peng, D., Li, J., Hu, Z., Wang, D., Gong, Z., & Fan, M. (2023). Surface-enhanced Raman Scattering (SERS) microbial sensor for fresh water acute toxicity monitoring. Microchemical Journal, 191, 108822.
[66] Xu, J., Xue, Y., Jian, X., Zhao, Y., Dai, Z., Xu, J., Gao, Z., Mei, Y., & Song, Y. Y. (2022). Understanding of chiral site-dependent enantioselective identification on a plasmon-free semiconductor based SERS substrate. Chemical Science, 13(22), 6550-6557.
[67] Gautam, R., Chaturvedi, D., Sil, S., Kuhar, N., Singh, S., & Umapathy, S. (2022, September). Characterization of Aggregating Agents towards Sensitive Optical Detection of Tryptophan Using Lab-on-a-Chip. In Photonics (Vol. 9, No. 9, p. 648). MDPI.
[68] A. Jaworska, K. Malek, K.M. Marzec, M. Baranska, Nicotinamide and trigonelline studied with surface-enhanced FT-Raman spectroscopy, Vibrational Spectroscopy 63 (2012) 469-476.
[69] J.L. Castro, J.F. Arenas, M.R. Lopez-Ramirez, J. Soto, J.C. Otero, Surface-enhanced Raman scattering of picolinamide, nicotinamide, and isonicotinamide: Unusual carboxamide

deprotonation under adsorption on silver nanoparticles, Journal of Colloid and Interface Science 396 (2013) 95-100.
[70] T. Pal, V. Anantha Narayanan, D.L. Stokes, T. Vo-Dinh, Surface-enhanced Raman detection of nicotinamide in vitamin tablets, Analytica Chimica Acta 368(1) (1998) 21-28.
[71] Hernandez, S., Perales-Rondon, J. V., Arnaiz, A., Perez-Estebanez, M., Gomez, E., Colina, A., & Heras, A. (2020). Determination of nicotinamide in a multivitamin complex by electrochemical-surface enhanced Raman spectroscopy. Journal of Electroanalytical Chemistry, 879, 114743.
[72] Hernandez, S., Perales-Rondon, J. V., Heras, A., & Colina, A. (2020). Electrochemical SERS and SOERS in a single experiment: A new methodology for quantitative analysis. Electrochimica Acta, 334, 135561.
[73] M. Kang, S.-G. Park, K.-H. Jeong, Repeated Solid-state Dewetting of Thin Gold Films for Nanogap-rich Plasmonic Nanoislands, Scientific Reports 5 (2015) 14790.
[74] N. Leopold, S. Cîntă-Pînzaru, M. Baia, E. Antonescu, O. Cozar, W. Kiefer, J. Popp, Raman and surface-enhanced Raman study of thiamine at different pH values, Vibrational Spectroscopy 39(2) (2005) 169-176.